LIVE IMAGING OF SUBCELLULAR PHOSPHATE POOLS IN PLANTS

A Dissertation

by

PALLAVI MUKHERJEE

Submitted to the Office of Graduate and Professional Studies of
Texas A&M University
in partial fulfillment of the requirements for the degree of

DOCTOR OF PHILOSOPHY

Chair of Committee,	Wayne K.Versaw
Committee Members,	Thomas D. McKnight
	Kathryn Ryan
	Astrid Volder
Head of Department,	Thomas D. McKnight

December 2013

Major Subject: Biology

ABSTRACT

Plants modulate photosynthesis and the subsequent fate of fixed carbon throughout each day to ensure that immediate carbon needs are met and that sufficient stores are available for the coming night. Although these processes are restricted to chloroplasts they must be tightly coordinated with metabolic pathways in the surrounding cytosol and ultimately, in distant cells within nonphotosynthetic parts of the plant. Inorganic phosphate (Pi) is a key determinant of metabolic status, and I hypothesize that the transport of inorganic phosphate (Pi) between the chloroplast and cytosol integrates metabolism in these cell compartments. PHT2;1 and PHT4;4 are unrelated Pi transporters that localize to the chloroplast inner membrane. Although I predicted that these proteins would be functionally redundant, the corresponding loss-of-function mutants exhibit opposite phenotypes with respect to biomass and starch accumulation. Based on these observations, I hypothesize that PHT2;1 and PHT4;4 transport Pi in opposite directions and that these proteins provide fine-tuning of Pi levels in the chloroplast. Because no suitable analytical technique existed to address this hypothesis I developed and optimized a series of genetically encoded fluorescent Pi biosensors for use in live plants. I confirmed that these biosensors could be targeted to different cell compartments and confirmed their utility for monitoring Pi concentrations in the cytosol and plastid stroma.

DEDICATION

To my Maa, Smt. Geeta Mukherjee and father, Shri. Dilip Mukherjee, I owe my life and dreams. Without their support and encouragement I could not have accomplished any of my goals in life. To my sister, Lipi Mukherjee, she is the personification of joy and happiness. She is my strength to stand against all odds. To my loving husband, Arnab Chattopadhyay, he completes me. It is because of his patience and support that I can excel.

To my brother in law, Rahul Joshi, he is a blessing to our family. His care and love has made us live again.

To all of my family and friends, their love helped me accomplish my goals.

ACKNOWLEDGEMENTS

Woods are lovely dark and deep, I have many promises to keep and miles to go before I sleep and miles to go before I sleep

-Robert Frost

I often heard these words of wisdom and blessings from my Maa; they kept me moving throughout the good and hard times. I would like to thank everyone who contributed to successful completion of this work. It is my pleasure to convey my gratitude to all of them in my own small way.

I give my sincere thanks to the person who has always been there to support, encourage and advise me, my P.I., Dr. Wayne Versaw. I owe a lot to him for teaching me the knits and grits of science. His constant encouragement to explore and experiment gave me the freedom required of an independent researcher. There were times when he pepped me up, calmed me down, and commended me for my efforts to bring the best in me. Thanks Dr. Versaw for being an oasis of encouragement and support.

I extend my heartfelt thanks to all my committee members Dr. McKnight, Dr. Ryan and Dr. Volder, for their encouragement, guidance and valuable input toward this work. I give special thanks to Dr. McKnight for his guidance through lab meetings, and for making conferences memorable with his wonderful treats. I admire his versatility.

My sincere thanks to Dr. Lockless and Dr. Garcia for helping me with their scientific vision and teaching me new skills. They have been a great source of inspiration.

I want to thank my colleague and friend Sonia, for being a wonderful lab mate. I will never forget the help and support I got from her. I thank Kranthi for always helping me with troubleshooting and giving me new ideas for making my work better. I had a great time working with Amanda, Lyndsay, Sharidon and John, the very productive undergrad team in our lab.

Friends are the soul of life. I am lucky to have friends like Priti and Arpita who were always there by my side no matter the situation. Thanks Shrinidhi, Maithereyi and Hema. I have no words to describe your selfless love and care; it is a blessing to have friends like you.

I have been lucky to be surrounded with very good and helping people. Thanks Tiffany, Sachi, Wang, Anjali, Kat, Jenny, Phil, Andy, Veria, Yichun, Paola, Xin, Xiaoyan, Shian, Niki and Vicky. Thanks to the wonderful Bio-Tamu Indian friends, the hangouts made me feel like I was home. Thanks Sachi for making me laugh with your witty comments.

It could be said that if a whole village is needed to raise a child then a whole faculty is needed to raise a Ph.D. I thank all of the faculty and staff for their support. Thanks Kay and Dr. Lekven for your time to listen to me and advise me to take the right action. Thank you Stan for always helping me with microscopy. Thanks Dr. Thomas for the “Kettle-boilers”, despite breaking three of them. You were generous to get replacements. I will never forget this generosity.

I am thankful to my wonderful mother-in-law and extended family for their patience and love. I am amazed by their stoic attitude and potential to share love.

Thanks to my cousins, Probalda, Joydeep, Bishwadeep and their lovely better halves. It's a privilege to have such loving and caring people as a part of my family. Thanks "Aanya" for adding those smiles to my life.

I acknowledge the support and love from the Los Angeles group of friends. Thanks Vijay, Bhumi, Tina, Mahavir, Harpreet and Shubha for making me feel so much loved.

My family is my strength, my motivation to live and do better. I feel I have the best family in the world. What ever I am I owe to my family. Thanks Maa, you are my soul and reason for existence. Thanks Baba for having faith in me and to let me be what I wanted to be.

Thanks Arnab, for withstanding my mood swings, tantrums and being there for me. I thank you for all the goodness that you brought into my life.

Munu and Rahul you guys are my "chokher moni" and I can't emphasize more that you both are indispensible part of my life.

I will always be proud to be an "Aggie". Memories of Texas A&M University will always be with me.

TABLE OF CONTENTS

LIST OF FIGURES

LIST OF TABLES

CHAPTER I

INTRODUCTION AND

LITERATURE REVIEW

Phosphate Is Essential for Plants

Phosphate (Pi) is an essential macronutrient for all living organisms, but its availability is often the limiting factor for plant growth. Plants accumulate Pi to about 0.2% of the their total dry weight (Schachtman et al., 1998), and it is used for variety of biological, structural and metabolic functions. It is a structural component of organophosphates like DNA and RNA, multifunctional nucleoside triphosphates like ATP, and phospholipids that constitute cell membranes (Bieleski, 1973). It also serves as a key regulator of many metabolic pathways and enzymatic reactions. Of prime importance to plants, Pi plays a major role in photosynthesis, both as a substrate for ATP synthesis via photophosphorylation and as a regulator for the partitioning of carbon to either sugar or starch (Marschner et al., 1996).

Phosphate Homeostasis and Pi Transporters

Maintaining the Pi balance in subcellular compartments is essential for normal functioning of the cells (Mimura, 1999). As Pi is crucial for cell growth, plants regulate the concentration of Pi by controlling the uptake, redistribution to various cell compartments, and storage (Raghothama, 1999). Oftentimes the Pi levels in soil are inadequate for normal plant growth. The concentration of orthophosphate, the only form

of phosphorus taken up by plants, was estimated to be only 10 μM in the soil solution (Bieleski, 1973). Orthophosphate also tends to form complexes or insoluble salts with other elements like iron, calcium and aluminum present in the soil, thus making it difficult for the plants to assimilate Pi.

Plants have various mechanisms to counteract the problems of low availability of Pi from the soil; this includes architectural changes in root (increase in lateral roots and root hairs, formation of proteiods or clustered roots, making mycorrhizal associations), biochemical changes (secretion of organic acids and phosphatases, remobilization of phosphates from vacuole and re-translocation of Pi from older leaves to younger leaves) (Robinson, 1994; Lynch, 1995; Raghothama, 1999; Abel et al., 2002; Versaw and Harrison, 2002) and molecular changes (up-regulation of the genes involved in uptake and distribution of Pi, like Pi transporters) (Mimura, 1995; Rausch and Bucher, 2002). As a first response to limited Pi condition, plants remobilize Pi stored in other compartments. This includes breaking down the intermediates and macromolecules that contain Pi. The vacuole is the main organelle that stores Pi. In Pi deficit conditions, Pi supply from the vacuole can only serve to maintain Pi balance in cytoplasm for a short period of time (Woodrow et al., 1984; Loughman et al., 1989; Mimura, 1999). Experiments with sequestered Pi have shown that the supply of Pi from vacuole cannot meet cytosolic demands due to a very slow exchange rate. Also, the import and export activities from vacuole to cytosol are not well understood. Regardless of these mechanisms, only the Pi transporters can mediate efficient uptake, distribution and re-translocation to different subcellular compartments (Mimura, 1995; Raghothama, 1999).

Thus, Pi transport across the membrane is essential for maintaining the homeostasis in plants (Mimura, 1999; Raghothama, 1999; Guo et al., 2008b).

Fine-tuning of Pi levels in the cell is achieved by a controlled exchange of Pi between various cells and subcellular compartments (Smith et al., 1990; Smith and Stitt, 2007). In experiments with isolated chloroplasts it was demonstrated that Pi levels in the chloroplast and cytosol not only affect photosynthesis but also the partitioning of carbon to sucrose or starch (Flügge and Heldt, 1984; Flügge, 1999). The details of this process will be discussed later. Pi levels inside the chloroplast may also influence complex metabolic networks independent of photosynthesis (Mimura, 1999). Persisting conditions of Pi deficiency give rise to a Pi limited condition that can limit photosynthesis (Sharkey, 1985; Sivak and Walker, 1986; Walker and Sivak, 1986). Hence, regulation of Pi levels in plastids like chloroplasts is important for plant metabolism (Plaxton and Carswell, 1999; Poirier and Bucher, 2002).

Kinetic and molecular studies showed that there are several Pi transporters involved in the transport of Pi across the cellular membranes (Flügge, 1998; Ferro et al., 2002). Depending on the plant metabolic needs, Pi concentrations are adjusted within subcellular compartments by selective transport of Pi across the membrane. There are five families of Pi transporters based on the sequence similarities: PHT1 (plasma membrane), PHT2 (plastid inner envelope), PHT3 (mitochondrial inner membrane) (Rausch and Bucher, 2002), PHT4 (plastid inner envelope and thylakoid and Golgi membrane) (Roth et al., 2004; Guo et al., 2008a; Cubero et al., 2009), and pPT (plastid inner envelope). These transporters will be discussed in more detail in later sections of

this thesis. One of aspect of the current study is to understand Pi homeostasis and functions of Pi transporters related to plastids.

Plastid Biology

A special feature of plant cells is that they contain plastids, organelles that are the site of many metabolic processes including photosynthesis, synthesis of fatty acids and assimilation of nitrogen (Flügge, 1999). Plastids can be categorized into two major groups: 1) plastids that have chlorophyll and are capable of photosynthesis, and 2) non-photosynthetic plastids that serve as storage sites for oil (elaioplasts) or starch (amyloplasts) (Neuhaus and Emes, 2000; Lopez-Juez and Pyke, 2005).

Plastids are derived from proplastids present in meristematic cells. As non-photosynthetic plastids lack chlorophyll, these cannot fix carbon or produce ATP like photosynthetic plastids. Thus, these plastids import carbon in the form of Glc-6P and ATP as an energy source from the cytosol to carry out biosynthetic reactions (Kammerer et al., 1998). To import ATP, nucleotide transporters (NTTs) catalyze the exchange of stromal ADP for cytosolic ATP (Reiser et al., 2004; Reinhold et al., 2007). A major need for ATP is the oxidative phase of the pentose phosphate pathway that generates important precursors for biosynthesis of purines and aromatic compounds (Kammerer et al., 1998; Lejay et al., 2008). In contrast, photosynthetic plastids (chloroplasts) make ATP by photophosphorylation and fix carbon through the Calvin cycle (Fig. 1).

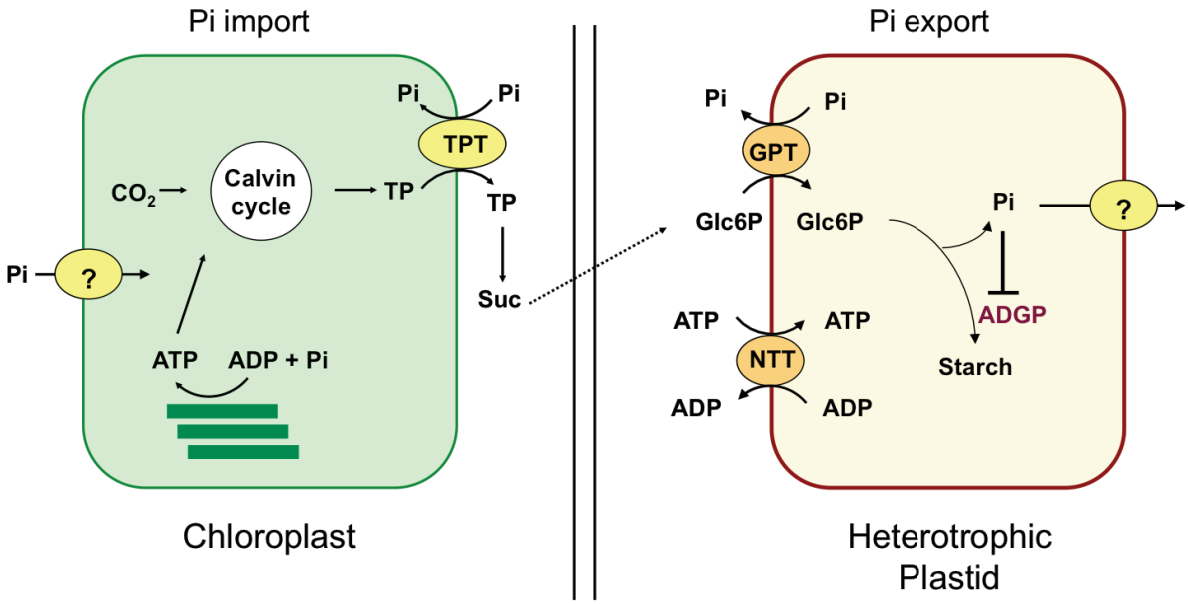

Figure 1. Pi transport processes in chloroplast and root plastids. TP, triose phosphate; GPT, glucose 6- Pi transporter; NTT, nucleotide transporter. Chloroplast import Pi from cytosol to synthesize ATP, which fuels the Calvin cycle for fixation of carbon. Sugars and ATP are exported from the chloroplast and are used by heterotrophic tissues. Exchange of ATP/ADP via the NTT transporters in the heterotrophic plastids results in net gain of one Pi in the plastids. As excess of Pi causes allosteric hindrance to enzyme ADP-glucose phosphorylase (ADGP), the heterotrophic plastids must get rid of excess of Pi via unidentified Pi transporter.

Chloroplast Phosphate Transport and Transporters

Chloroplasts are the primary biosynthetic center for plants. This organelle is bound by a double membrane or envelope. The inner membrane is the permeability barrier and has several proteins that are known or predicted to catalyze Pi transport between the cytosol and stroma.

Pi transport in plastids is often attributed solely to members of the pPT family. Members of the pPT (plastdic phosphate translocator) family are antiporters known to mediate Pi transport across the inner envelope of plastids in exchange for phosphorylated C3, C4 or C6 carbon compounds (Kammerer et al., 1998; Flügge, 1999; Neuhaus and Emes, 2000; Knappe et al., 2003; Weber, 2004). TPT (Triose Phosphate Translocator) was the first member of the pPT family to be identified and cloned from plants. It is expressed only in the photosynthetic tissues (Flügge et al., 1989; Flügge, 1999). The transport activities of TPT as a Pi link between the cytosol and chloroplast was demonstrated in transgenic potato with an antisense suppressor for *tpt* (Riesmeier et al., 1993).

TPT mediates the efflux of triose phosphate (triose-P) (end product of photosynthesis) from the stroma for the exchange of the cytosolic Pi (Heldt and Sauer, 1971). Pi levels in the stroma and the cytosol play a crucial role in determining the partitioning of the triose-P into sucrose or starch. In the cytosol, sucrose is synthesized from the triose-P, and the Pi released in this process is returned to the chloroplast for the synthesis of ATP (Gibon et al., 2004; Smith and Stitt, 2007). Sucrose is the main source of carbon distributed to all parts of the plants including the heterotrophic parts like roots.

As the demand for sucrose goes down during the day, sucrose formation declines and the Pi concentration in the cytosol also declines. This limits the export of triose-Pi from the stroma. As a consequence, stromal Pi levels also drop and triose-P is partitioned toward synthesis of starch. Biosynthesis of starch liberates Pi from organic compounds and thus serves as a mechanism to recycle Pi for continued photosynthesis. The presence of high Pi concentrations in the stroma is inhibitory for the formation of starch because Pi acts as an allosteric inhibitor for the enzyme ADP-glucose phyrophosphorylase(Sheu-Hwa et al., 1975; Preiss, 1982; Nielsen et al., 1998; Ballicora et al., 2004). This enzyme regulates the first committed step of the starch synthesis; it converts glucose-1-phosphate and ATP to ADP-glucose and pyrophosphate (PPi). However the *tpt* mutants do not show any growth defect under normal growth conditions (Barnes et al., 1994; Schneider et al., 2002; Walters et al., 2004). These plants do exhibit increased starch synthesis and turnover rates to compensate for the defect in carbon allocation, which suggests that compensatory or redundant mechanisms also exist for the coupled defect in Pi import. Interestingly, other members of the pPT family like phosphoenolpyruvate/Pi translocator (PEP) and xylulose 5-phosphate/Pi translocator (XPT) in chloroplasts, and glucose-6-phosphate/Pi translocators (GPT) in heterotrophic plastids, catalyze export of Pi in exchange for cytosolic metabolites that serve as precursors for biosynthetic processes in the stroma (Muchhal et al., 1996; Fischer et al., 1997; Kammerer et al., 1998; Flügge, 2003).

Plastids also have Pi transport activities that are not coupled to carbon exchange. This kind of an exchange has been termed as “unidirectional” Pi transport (Neuhaus and

Maass, 1996; Neuhaus and Wagner, 2000). To date, six candidates of unidirectional transporters have been identified in Arabidopsis, which include the members of the PHT2 family (PHT2;1) and PHT4 family (five members). These two families are unrelated to each other and also do not show any resemblance to the members of the pPT family (Ferro et al., 2002). In Arabidopsis, the PHT2 family comprises a single protein, PHT2;1, which localizes to the inner membrane of the chloroplast. Functional characterization of this transporter was done in yeast, which demonstrated that it is a low affinity Pi transporter that is dependent on a proton gradient, suggestive of H^+/Pi symport. (Daram et al., 1999; Versaw and Harrison, 2002). PHT2;1 shares similarity to mammalian type III Na+/Pi symporters found in fungi and mammals. Homologs of PHT2;1 are also reported to be present in spinach, medicago, potato. Null mutants of this transporter have reduced size and low Pi content in leaves. Although it has not been demonstrated directly, the low Pi levels may limit photosynthesis (Sivak and Walker, 1986; Versaw and Harrison, 2002).

The PHT4 family of Pi transporters was found by data mining of the Arabidopsis genome. This family shares similarity to the structurally distinct mammalian type I Na^+/Pi symporters. It was also found that these proteins had N-terminal sequences that might serve as plastid targeting sequences (Ferro et al., 2002; Zhao et al., 2003; Rausch et al., 2004). The Arabidopsis PHT4 family consists of six members (PHT4;1-PHT4;6). Subcellular localization studies showed that five members (PHT4;1-PHT4;5) are located in plastids. PHT4;6 is located in the Golgi apparatus (Table I). Yeast expression experiments demonstrated that all members of the PHT4 family mediate Pi transport,

and like PHT2;1, Pi transport is H^+-dependent. Interestingly, PHT4;1 catalyzed Na^+-dependent Pi transport when expressed in *E. coli* , and in plants, PHT4;1 is located in the thylakoid membrane of the chloroplast (Ruiz Pavón et al., 2008). Promoter-Gus expression studies revealed that PHT4;3 and PHT4;5 are restricted to leaf phloem (Guo et al., 2008b). In contrast, PHT4;2 is restricted to heterotrophic tissues. Null *pht4;2* mutants have significantly reduced starch accumulation, but are significantly larger than wild-type plants (Irigoyen et al., 2011). Further investigations are required to know the transport mechanism and direction of the Pi transport.

Table I. List of PHT4 family members.

PHT4 GENE FAMILY MEMBER	LOCUS	Protein subcellular location	References
PHT4;1	At2g29650	Thylakoid membrane	(Ruiz Pavón et al., 2008; Guo et al., 2008b)
PHT4;2	At2g38060	Root plastids	(Irigoyen et al., 2011)
PHT4;3	At2g46980	Phloem	(Guo et al., 2008b)
PHT4;4	At2g00370	Chloroplast inner membrane	(Guo et al., 2008b)
PHT4;5	At2g20380	Phloem	(Guo et al., 2008b)
PHT4;6	At2g44370	Golgi	(Guo et al., 2008b)

Genetic and biochemical studies to discern the roles of PHT2;1 and PHT4;4 in chloroplast Pi homeostasis are described in chapter 3.

In vivo Pi Measurement

To better understand the mechanisms governing cellular Pi homeostasis, and to understand the roles of individual Pi transporters it is necessary to assess Pi levels in separate subcellular compartments in real time. This is a very challenging task because the concentration of Pi in each compartment can be variable (Vidal et al., 1997), and there are no suitable methods for monitoring changes in Pi concentration in live cells in real time. There have been conflicting views over the concentration of cytosolic Pi. It has been reported that cytosolic Pi concentration falls from 5 mM under normal growth conditions to about 0.2 mM under Pi-deficit conditions (Rausch and Bucher, 2002). But in another study it was shown using NMR that under normal conditions (sufficient Pi supply) the concentration of Pi in the cytosol is 60-80 μM, and with a Pi deficiency it could drop down to as low as 15 μM (Pratt et al., 2009). My current work will address this issue in chapters 2 and 4.

Current methods to measure Pi concentration in real time include nuclear magnetic resonance (NMR) and non-aqueous fractionation (NAF). Quantification of phosphorylated materials in plant matter by ^{31}P NMR was first reported in root tissues (Ratcliffe and Shachar-Hill, 2001). The spectra can distinguish abundant phosphomonoesters, nucleoside triphosphates and nucleoside diphosphate sugars. NMR is non-destructive (at the cellular level) so it is possible to capture a series of *in vivo* spectra from the same sample follow the time course of metabolic changes in plants. The major disadvantages of NMR are that it lacks cellular resolution and can only distinguish cell compartments with large differences in pH (Desmoulin et al., 1987; Vidal et al.,

1997; Martel et al., 2002; Looger et al., 2005). For NAF, tissues are frozen in liquid nitrogen, homogenized, lyophilized and the resulting fragments are then separated by density centrifugation in an organic solvent mixture. The distribution of marker enzymes and metabolites can then be used to define the subcellular distribution of Pi (Gerhardt and Heldt, 1984; Gerhardt et al., 1987; Sharkey and Vanderveer, 1989). Disadvantages of this method are that it is a labor intensive, very sensitive to moisture, lacks cellular resolution and is prone to artifacts (Sharkey and Vanderveer, 1989; Geigenberger et al., 2011).

FRET-based sensors are powerful alternatives to NMR and NAF for measurement of metabolites with subcellular resolution in live cells (Lalonde et al., 2005). FRET sensors have of two fluorophores (e.g., variants of GFP like CFP and YFP) that are linked by a polypeptide that can bind the target molecule. Ligand binding causes a change in conformation, which can be detected by measuring the change in FRET (Fig. 2). FRET is Forster/fluorescence resonance energy transfer, where the non-radiative energy transfer takes place from the donor to the acceptor molecule through dipole-dipole coupling when the donor molecule is excited (Förster, 1948; Okumoto et al., 2008). This energy transfer can be measured in terms of FRET efficiency (E), which is defined as the fraction of photons that is absorbed by the donor molecule and transferred to acceptor.

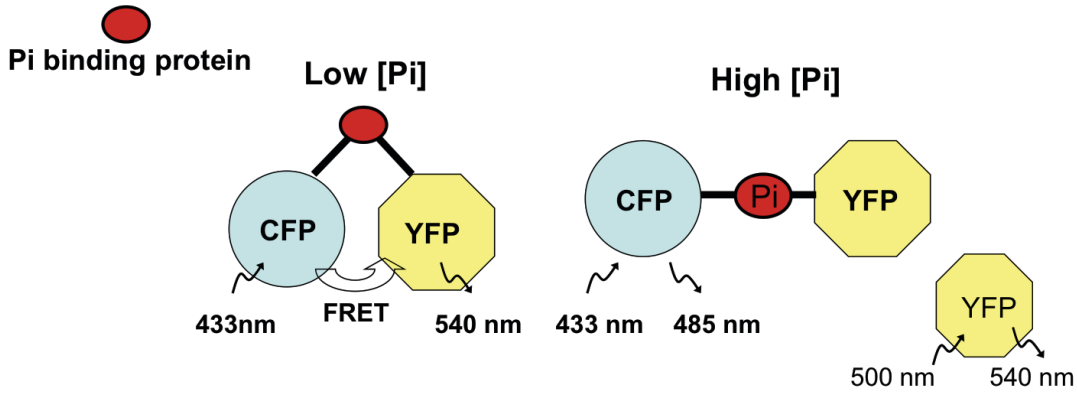

Figure 2. Model for a FRET-based Pi sensor. A Pi binding protein is fused to two fluorescence proteins, CFP and YFP. In the absence of Pi, FRET occurs between CFP and YFP. Pi binding causes a conformational change that disrupts FRET. Ratiometric analysis of YFP/CFP emission is conducted to detect changes in Pi concentration. CFP, cyan fluorescent protein; YFP, yellow fluorescent protein; FRET, Förster/ Fluoresence resonance energy transfer.

The utility of FRET sensors for use *in vivo* was first described for the measurement of calcium (Persechini et al., 1997). Many variants of this sensor with improved ligand interaction and sensitivity have been used for imaging of live cells to track calcium changes (Krebs et al., 2012). For other metabolite sensors, PBPs (periplasmic binding proteins) from bacteria have been used to provide ligand specificity. This large family of binding proteins includes proteins that are specific for the binding of amino acids and sugars (Tam and Saier, 1993). For example, the FLIPsuc sensor has been used to monitor sucrose in cells (Lager et al., 2006). Other FRET sensors include: Clomelion for detection of halides (Jose et al., 2007), Cameleon for

detection of calcium (Rincon-Zachary et al., 2010) , FLIPglu for glucose detection (Deuschle et al., 2006), FLIPmal for maltose detection (Kaper et al., 2008) and a FRET reporter for detection of glutamine in cells (Yang et al., 2010). Recently FRET-based biosensors called "pHusion" have been used for measurement of intra and extracellular pH in plants (Gjetting et al., 2012). Similarly, for detection of Pi concentration in cells Gu.*et.al* developed FLIPPi constructs. This sensor is capable of detecting changes in Pi concentration in COS7 cells (Gu et al., 2006). However, we found that sensor is not suitable for detection of Pi in plants.

In the current study, FLIPPi sensors have been optimized to monitor Pi in live plants. Details of this work are described in chapter 2. The research presented in this thesis describes novel tools and genetic resources necessary to understand mechanisms involved in Pi homeostasis.

CHAPTER II

LIVE IMAGING OF SUBCELLULAR PHOSPHATE POOLS IN PLANTS

Introduction

Inorganic phosphate (Pi) is an essential macronutrient. It has vital roles in energy conversion, signal transduction, enzyme regulation, and it is a component of numerous metabolites and macromolecules, including nucleic acids and phospholipids. Fulfilling these fundamental roles is particularly challenging for plants because the supply available from soil is often limited (Schachtman et al., 1998; Raghothama, 1999). Once Pi is acquired, plants must coordinate its distribution to different cell types and compartments. Distribution is affected by diurnal changes in metabolic demand as well as environmental conditions (Plaxton and Carswell, 1999; Karley et al., 2000; Poirier and Bucher, 2002). Pi concentrations in the plastid stroma and cytosol regulate photosynthesis and carbon partitioning (Stitt et al., 1988; Sharkey and Vanderveer, 1989) and Pi stored in the vacuole serves as a reservoir to buffer the cytosol during prolonged deprivation (Mimura, 1999).

Some of the transporters that mediate the acquisition of Pi and its subsequent transfer between cell compartments have been identified, and these are classified within five distinct families: PHT1 (plasma membrane), PHT2 (chloroplast inner envelope), PHT3 (mitochondrial inner membrane), PHT4 (plastid inner envelope, chloroplast thylakoid and Golgi) and pPT (plastid inner envelope) (Takabatake et al., 1999; Mudge et al., 2002; Versaw and Harrison, 2002; Ruiz Pavón et al., 2008; Guo et al., 2008a;

Weber and Linka, 2011). Our understanding of how Pi transport activities throughout the plant are coupled with sensing, signaling and metabolic recycling activities (Rouached et al., 2010; Chiou and Lin, 2011; Plaxton and Tran, 2011; Jain et al., 2012) is limited by the inability to assess Pi concentrations with high spatial and temporal resolution *in vivo*. For example, X-ray microanalysis can distinguish amounts of Pi present in different cells, but has limited subcellular resolution and cannot be conducted with live plants (Karley et al., 2000). Nonaqueous fractionation and ^{31}P-NMR probe some of the subcellular Pi pools, but these methods lack cellular resolution and are either destructive or cannot be conducted with intact plants or organs (Gerhardt and Heldt, 1984; Rebeille et al., 1984; Pratt et al., 2009).

Genetically encoded fluorescent sensors have proven to be powerful tools for measurements of metabolites and ions *in vivo* because their expression and subcellular targeting can be manipulated and fluorescence imaging is nondestructive (Lalonde et al., 2005; Okumoto et al., 2008; Okumoto et al., 2012). Sensor proteins are fusions of a ligand-binding domain or protein with one or two fluorescent proteins, e.g., GFP and related variants. Sensors with a single fluorescent protein report ligand-dependent changes in conformation as changes in fluorescence intensity, whereas sensors with two fluorescent proteins can yield changes in Förster (or fluorescence) resonance energy transfer (FRET), which can be quantified through ratiometric imaging. FRET-based sensors have been used in live plants to assess a variety of analytes including glucose, maltose, sucrose, glutamine, calcium, zinc and pH (Deuschle et al., 2006; Chaudhuri et al., 2008; Kaper et al., 2008; Rincon-Zachary et al., 2010; Chaudhuri et al., 2011; Adams

et al., 2012; Gjetting et al., 2012; Krebs et al., 2012; Gjetting et al., 2013).

Gu et al. (Gu et al., 2006) engineered FRET-based sensors for Pi named FLIPPi (fluorescence indicator protein for Pi) sensors that consist of a *Synechocccus* Pi binding protein fused to eCFP and eYFP, and confirmed the utility of these sensors for monitoring Pi concentration in cultured animal cells. In this study, we modified and optimized FLIPPi sensors for use in plants and confirmed their utility for monitoring Pi in the cytosol and plastid stroma of live plants. To increase signal gain and reduce sensitivity to pH we substituted the eYFP component of a FLIPPi sensor with a circular permuted form of Venus (cpVenus) (Nagai et al., 2002; Nagai et al., 2004).

We next conducted a mutant screen to isolate a series of Pi binding affinity variants and confirmed the localization of candidate proteins engineered with and without an N-terminal plastid targeting sequence when expressed in Arabidopsis. Confocal microscopy coupled with ratiometric analysis or acceptor photobleaching revealed uniform changes in cytosolic Pi concentrations in root epidermal cells of plants that had been starved for Pi, and these changes were reversed by Pi replenishment. Steady-state cytosolic Pi levels were equivalent in plants supplied with a wide range of Pi concentrations, indicative of cytosolic buffering, but dropped when supply was reduced below a critical threshold. In addition, analysis of a plastid-localized sensor expressed in wild-type plants and in mutants lacking the PHT4;2 plastidic Pi transporter (Irigoyen et al., 2011) confirmed a role for this transporter in the export of Pi from root plastids. These results demonstrate the utility of cpFLIPPi sensors for real-time monitoring of Pi distributions with both cellular and subcellular resolution in live plants.

Results

In vitro calibration of FRET-based Pi sensors

In an initial attempt to monitor Pi distributions in live Arabidopsis plants we generated stable transgenic lines for two FLIPPi sensors, FLIPPi-200μ and FLIPPi-30m, that previously yielded robust Pi-dependent FRET responses with K_d values of 200 μM and 30 mM, respectively, when assayed *in vitro* (Gu et al., 2006). One of these sensors, FLIPPi-30m, also reported changes in cytosolic Pi concentrations in cultured animal cells. Constitutive expression of the sensor genes was directed from the *35S* promoter, and because no organellar targeting sequences were incorporated in the constructs the expressed sensor proteins were restricted to the cytosol. Independent transgenic lines for both sensors exhibited weak or highly variable fluorescence that diminished rapidly with plant age, suggestive of transgene silencing (Deuschle et al., 2006). Although signal intensity and stability improved when the sensors were expressed in an RNA-silencing mutant host, no changes in FRET were detected when plants were starved for Pi (data not shown).

We hypothesized that one or more attributes of the FLIPPi sensors limit their efficacy when used in plants. For example, subtle changes in cytosolic Pi concentrations would not yield a detectable response if the sensors have a low FRET signal gain or an affinity for Pi too far above or below the physiological concentrations. To explore these possibilities we first confirmed that purified FLIPPi-200μ and FLIPPi-30m sensor proteins yielded Pi-dependent FRET responses equivalent to those reported previously (Gu et al., 2006) (data not shown). We then examined FRET responses for the purified

proteins in a pseudocytosol medium (Messerli and Robinson, 1998; Feijó et al., 1999; Cardenas et al., 2008) to simulate *in vivo* conditions more closely than the buffer solution used for previous *in vitro* calibrations (Gu et al., 2006). In this case the FLIPPi-30m sensor yielded erratic FRET signals regardless of Pi concentration (data not shown), which may explain the absence of Pi-dependent FRET responses in the corresponding transgenic plants. In contrast, FLIPPi-200μ exhibited the expected Pi-dependent reduction in FRET, and the 190 μM K_d for Pi binding was nearly identical to that measured in buffer (Fig. 3). However, the maximum change in FRET ratio (R_{max}) was relatively small (Fig. 3) and the signal gain was very low over the 2.5-10 mM concentration range that encompasses estimates for cytosolic Pi (Rebeille et al., 1984; Stitt et al., 1988; Lee and Ratcliffe, 1993; Copeland and Zammit, 1994; Gout et al., 2011). Based on these results, we chose to focus our efforts on optimizing FLIPP-200μ.

Pi sensors with a circularly permuted Venus have enhanced FRET signal gain

Substitution of the YFP acceptor in a Cameleon FRET-based sensor for Ca^{2+} with a circularly permuted version of Venus (cpVenus) improved signal gain and stability and reduced acid sensitivity (Nagai et al., 2004). This modified sensor was then effective for monitoring Ca^{2+} dynamics in plants (Miyawaki et al., 1999; Shaner et al., 2005; Deuschle et al., 2006; Rincon-Zachary et al., 2010; Krebs et al., 2012). To test whether this manipulation would also enhance signal gain for a Pi sensor we replaced the eYFP portion of FLIPPi-200μ with cp173Venus, the same cpVenus variant used to improve the YC3.60 Ca^{2+} sensor (Nagai et al., 2004).

As shown in Fig. 3, the modified Pi sensor cpFLIPPi-200μ, had greater FRET ratios in the absence of Pi and at all concentrations tested. More importantly, the maximum change in FRET ratio (ΔR_{max}) was nearly 150% greater using the modified sensor (-1.08) compared to the original sensor (-0.44).

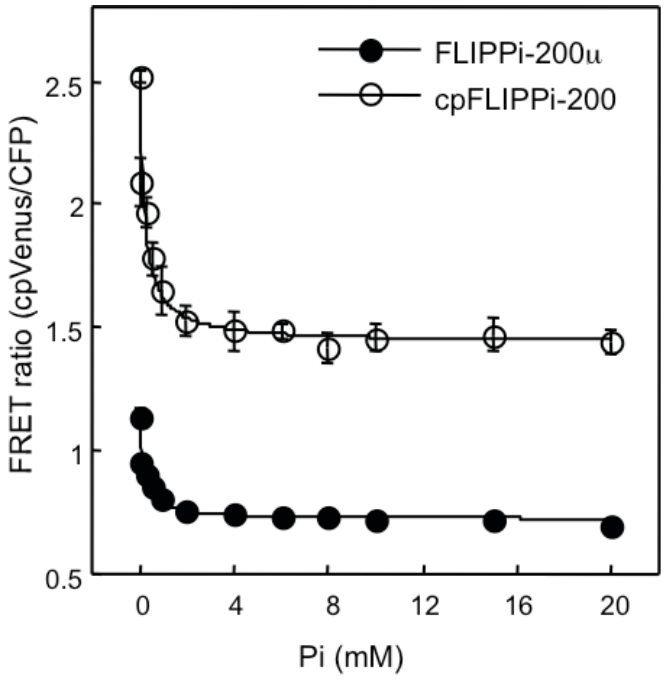

Figure 3. Replacing the YFP component of the FLIPPi-200μ sensor with a circular permuted version of Venus (cpVenus) enhanced FRET signal gain. Values shown are mean ± SE for three independent sensor protein preparations.

The emission spectra for cpFLIPPi-200μ (with CFP excitation) confirmed that this Pi-dependent response of this sensor was due to FRET (increase in CFP emission

directly coupled to a decrease in cpVenus emission) rather than unrelated changes, e.g., salt sensitivity, in the fluorescence intensities of either CFP or cpVenus (Fig. 4).

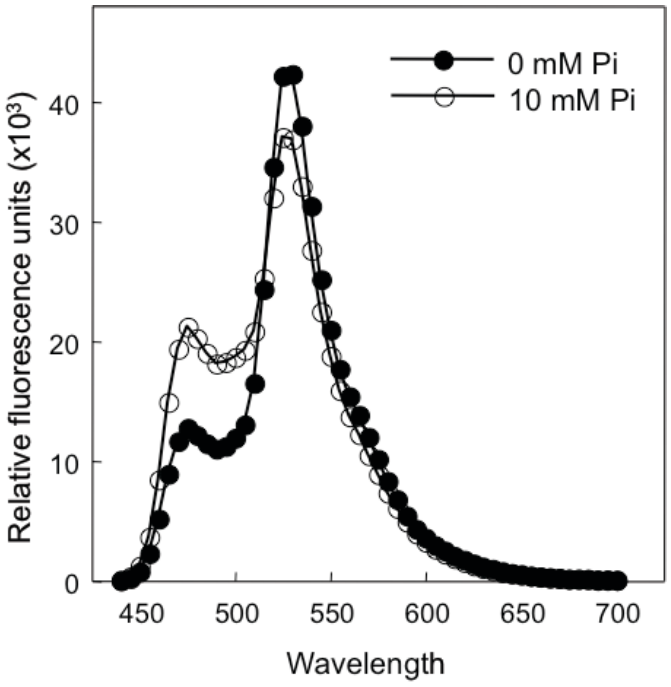

Figure 4. Emission spectrum of cpFLIPPi-200μ in pseudocytosol medium containing 0 and 10 mM Pi. The sensor was excited at 420 nm (CFP excitation). CFP emission is maximal at 480 nm and cpVenus emission is maximal at 540 nm. The Pi-dependent increase in CFP emission coupled with Pi-dependent decrease in cpVenus emission is indicative of FRET.

Mutant cpFLIPPi sensor variants with altered affinities for Pi

The large increase in maximum FRET signal gain observed with cpFLIPPi-200μ

had no significant effect on affinity for Pi. Consequently, the signal gain over the target concentration range of 2.5-10 mM remained low. This situation necessitated a mutant screen to obtain cpFLIPPi variants with binding affinities within the target concentration range.

To limit the scope of mutagenesis we used statistical coupling analysis (SCA), a sequence-based method for identifying protein residues or regions responsible for ligand binding affinity and potential allosteric sites (Lockless, 1999; Socolich et al., 2005). SCA was conducted with an alignment of the *Synechocccus* Pi binding protein (PiBP) sequence with 1020 of the most closely related protein sequences (PSI-BLAST e-score <1e-10) available from GenBank. We found that the region spanning amino acids 18-23 contained multiple coupled sites that map near the predicted Pi binding site (Fig. 5 and Fig. 6) and thus alterations in this region could change the binding affinity of the sensor protein.

We used PCR to introduce random mutations in the corresponding region of the cpFLIPPi-200μ plasmid clone. The mutant library was introduced into *E. coli,* and lysates of individual clones were screened for Pi-dependent FRET with the desired binding affinity. Eight candidate sensor mutants were identified and their Pi-dependent FRET responses were verified using the purified proteins (Table II). The K_d values ranged from 0.08 to 11 mM, which spans the predicted physiological range for the cytosol as well as the plastid stroma (Sharkey and Vanderveer, 1989; Tiessen et al., 2012).

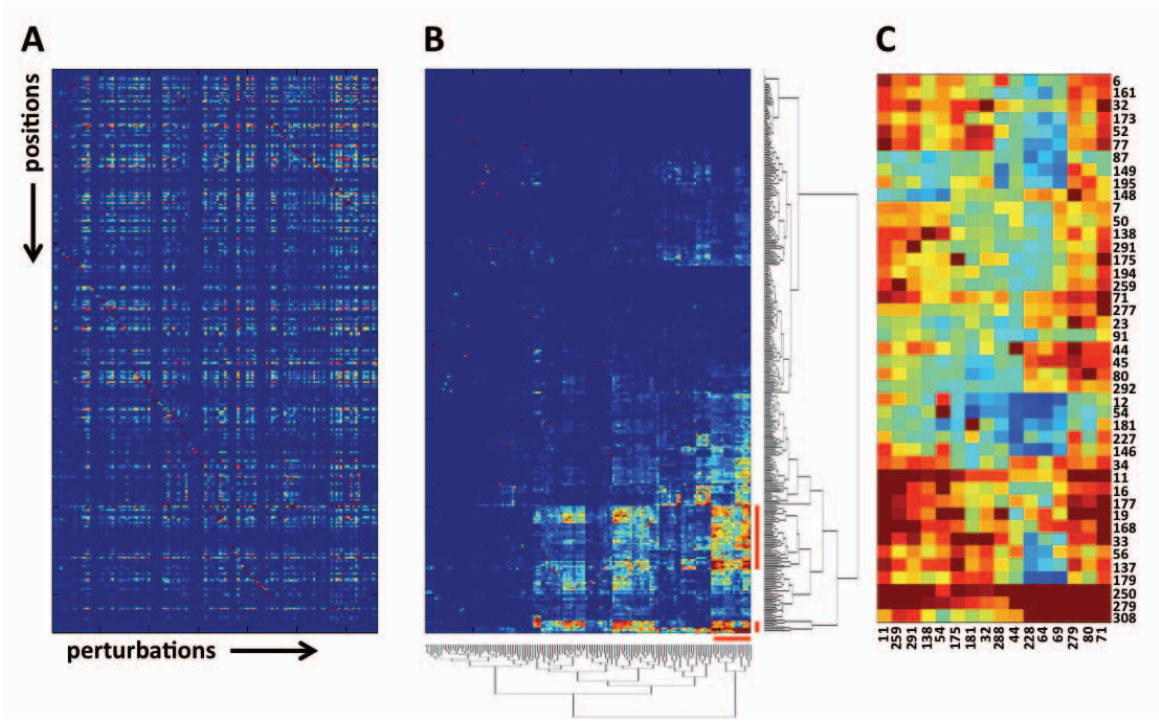

Figure 5. Statistical coupling analysis (SCA) reveals residues in the PiBP protein family likely to influence Pi binding. A, SCA matrix showing the statistical coupling values at each position (y-axis) after a perturbation is made at another position (x-axis). The color represents the coupling values from low (blue) to high (red). B. A 2-D clustering of the matrix shown in A is used to identify groups of positions and perturbations that co-evolve with one another. The red bar shows the clusters that are used for the final matrix. C, The final matrix of positions that represent the self-consistent cluster. These positions are mapped onto a structure in Figure 6.

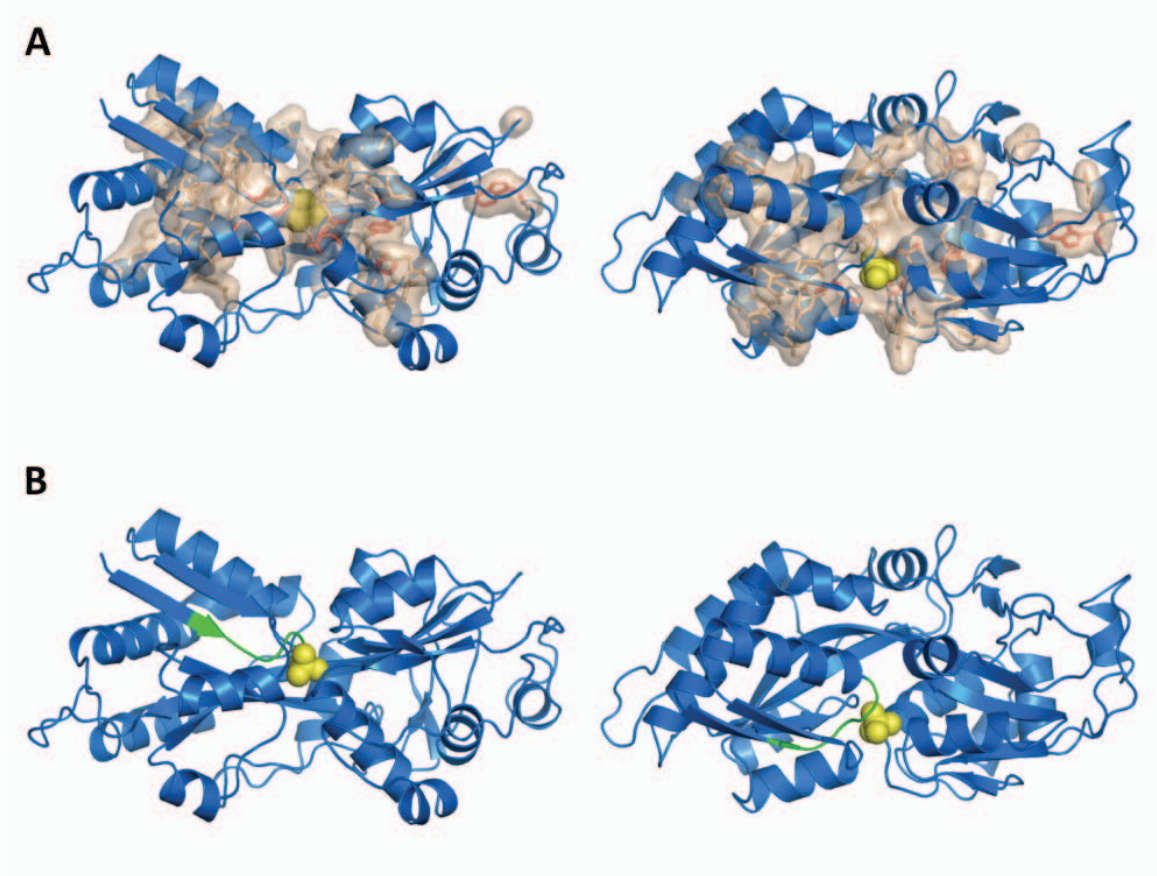

Figure 6. Mapping of co-evolving and mutated residues onto a PiBP structure (pdb1A40). The secondary structure is shown as a blue cartoon and the bound phosphate is yellow. The right figures are 90° rotations about the x-axis. A, Co-evolving and highly conserved positions are mapped onto the PiBP structure (encompassed by tan surface). The co-evolving amino acids are tan sticks and the highly conserved amino acids are red sticks. B, The mutated segment is shown in green and includes both highly conserved and co-evolving positions.

TABLE II. Pi sensor mutants

Sensor	K_d (mM)	ΔR_{max}	DNA sequence of *PiBP* cds	Protein sequence
cpFLIPPi-80u	0.08	-1.06	49 TCCG**tc**GC**t**GGC**t**CGACC**acc**GCG	17 S**V**AG**S**T**T**A
cpFLIPPi-200u	0.2	-1.08	49 TCCGGGGCGGGCGCGACCTTTGCG	17 SGAGATFA
cpFLIPPi-1.6m	1.6	-0.91	49 TCCG**cc**G**at**GGC**t**CGACC**a**T**c**GCG	17 S**AD**G**S**T**I**A
cpFLIPPi-3.5m	3.5	-0.43	49 TCCGG**c**GC**t**GGC**t**CGA**a**GT**c**TGCG	17 SGAG**SKS**A
cpFLIPPi-4.8m	4.8	-0.76	49 TCC**acc**G**at**GGCGCGACC**gcc**GCG	17 S**TD**GAT**A**A
cpFLIPPi-5.3m	5.3	-0.71	49 TCC**a**G**c**G**at**GGC**t**CG**t**CC**gtc**GCG	17 S**SD**G**SSV**A
cpFLIPPi-6.4m	6.4	-0.75	49 TCCGGGGCGGGCGCG**g**CCTTTGCG	17 SGAGA**A**FA
cpFLIPPi-11m	11.0	-0.45	49 TCC**atct**C**t**GGC**t**CG**t**CC**a**T**c**GCG	17 S**IS**G**SSI**A

Pi binding parameters were determined *in vitro*.

Specificity of cpFLIPPi sensors

To determine whether cpFLIPPi mutations that altered the affinity for Pi also affected specificity we examined the effect of other oxyanions, including organophosphates, on FRET signals. None of the sensors showed concentration-dependent FRET responses indicative of binding to sulfate or nitrate and the results for one sensor are shown in Fig.7A. Similarly, treatment with glycerol-2-phosphate and pyrophosphate, a phosphate ester and anhydride, respectively, yielded little or no FRET responses (Fig. 7B). These results suggest that the cpFLIPPi sensors have high specificity for Pi.

Effect of pH on Pi-dependent FRET responses

Our standard *in vitro* calibration assays and related tests for specificity were conducted at pH 7.5 to simulate the cytosol and plastid stroma (Demmig and Gimmler, 1983; Wu et al., 1991; Pratt et al., 2009; Gout et al., 2011)**.** Although the cytosol is tightly buffered at this pH, the chloroplast stroma can vary from pH 7 to pH 8 in

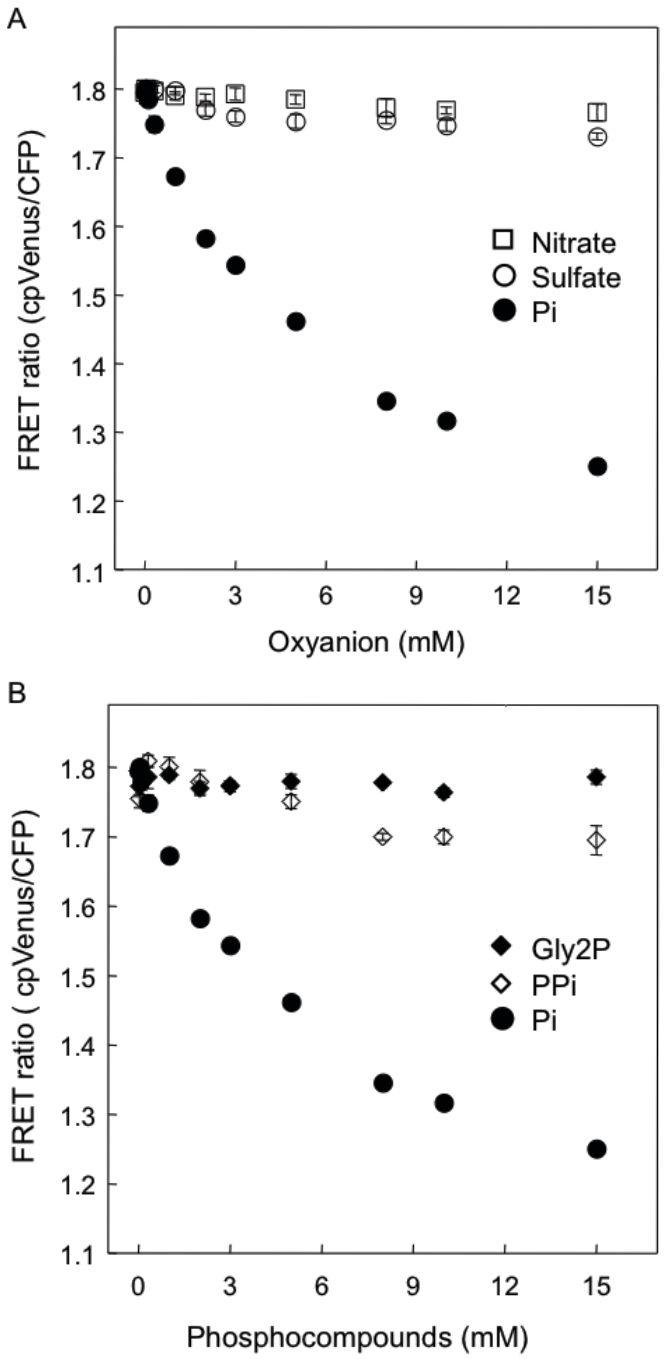

Figure 7. cpFLIPPi sensors have high specificity for Pi**.** A**,** FRET ratio response to nitrate, sulfate and Pi. B, FRET ratio response to glycerol-2-phosphate (Gly2P), pyrophosphate (PPi) and Pi. Values shown are mean ± SE for three independent sensor cpFLIPPi-5.3m protein preparations.

response to light (Demmig and Gimmler, 1983). Because one of our goals was to determine the utility of Pi sensors for monitoring plastidic Pi concentrations, we examined Pi-dependent FRET responses over this pH range for each of the cpFLIPPi sensors. We observed a consistent trend in which affinity decreased with increasing pH and results for one representative sensor are shown in Fig. 8. These apparent differences in affinity can be attributed almost entirely to the effect of pH on ionization of Pi with specificity for the monobasic form. However, differences in FRET signals measured in the absence of Pi (Fig. 8) suggest that pH also influences inherent FRET efficiency.

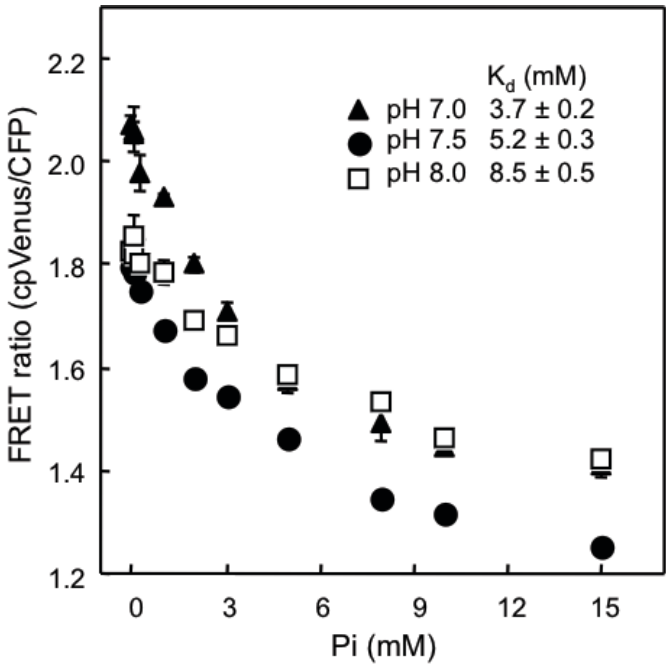

Figure 8. Effect of pH on Pi binding. The apparent binding affinity (K_d) decreases with increasing pH. Values shown are mean ± SE for three independent cpFLIPPi-5.3m sensor protein preparations.

Subcellular targeting of cpFLIPPi sensors

To test the fidelity of targeting cpFLIPPi sensors to the cytosol and plastid stroma of plant cells we constructed expression clones for each of the eight different cpFLIPPi sensors to yield proteins with and without an N-terminal RbcS chloroplast transit peptide (Lee et al., 2006). To avoid potential complications associated with the *35S* promoter, the Arabidopsis *UBQ10* promoter was used to drive constitutive expression at moderate levels (Norris et al., 1993; Geldner et al., 2009; Grefen et al., 2010). Constructs were introduced into the Arabidopsis RNA silencing mutant *sgs3-13* (Kumakura et al., 2009) to minimize potential loss of fluorescent signals due to post-transcriptional gene silencing (Deuschle et al., 2006). Protoplasts were prepared from the leaves of 5-week-old plants and fluorescence signals were viewed with confocal microscopy. Representative results shown in Fig. 9 confirmed that addition of the RbcS chloroplast transit peptide was sufficient to target sensors to plastids (co-localization with chlorophyll autofluorescence), whereas unmodified sensors were excluded from plastids and appeared to be restricted to the cytosol.

cpFLIPPi sensors report changes in cytosolic Pi concentrations in intact Arabidopsis plants

Live cell imaging using a confocal microscope equipped with a beam splitter for simultaneous dual emission fluorescence was used to test the functionality of cpFLIPPi sensors for reporting changes in cytosolic Pi concentrations. Untransformed plants and transgenic plants expressing eCFP alone and cpVenus alone were imaged each day to

correct for fluorescence background and spectral bleed-through respectively. T2 generation transgenic seedlings were grown for 5 days in hydroponic medium containing 0.5 mM Pi then placed in an imaging chamber containing the same medium.

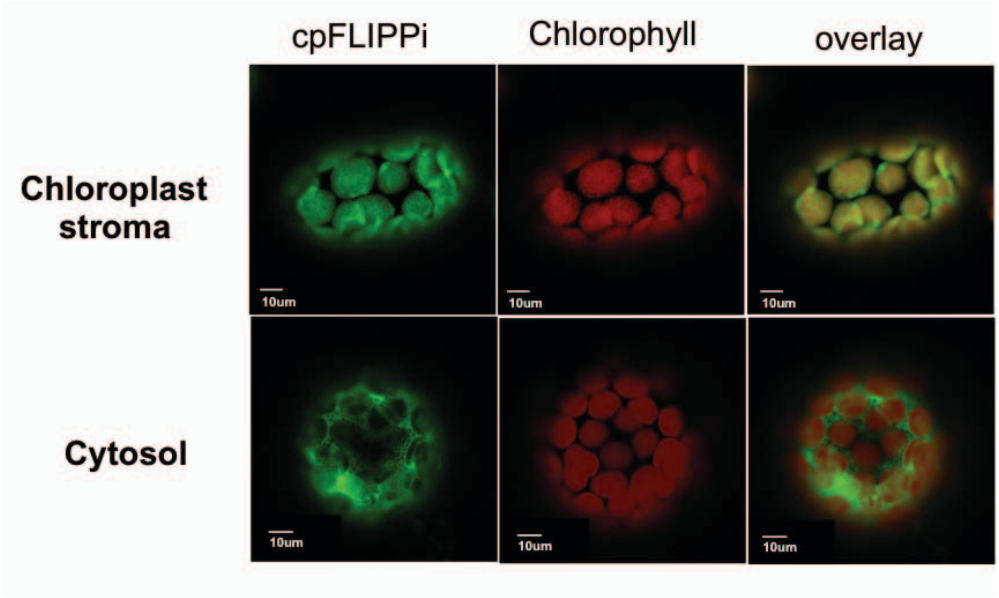

Figure 9. Pi sensors can be targeted to different cell compartments. Plastid and cytosol-targeted versions of the cpFLIPPi-6.4m sensor were introduced into the *sgs3-13* RNA silencing defective mutant and protoplasts were imaged. The green signals indicate directly excited cpVenus and the red signals indicate chlorophyll autofluorescence.

Images for multiple epidermal cells within the root transition zone were captured from at least six independent seedlings of each genotype tested to establish the steady-state baseline for the FRET ratio under this Pi-sufficient growth condition. The same

seedlings were then transferred to medium that lacked Pi and imaged again after 24 hours of Pi starvation. The duration of Pi starvation was limited to avoid morphological changes or cell death associated with more severe Pi deprivation (Sánchez-Calderón et al., 2005), and cell viability tests with SYTOX orange (Truernit and Haseloff, 2008) confirmed the viability of imaged root cells (data not shown). Separate experiments demonstrated that this Pi starvation regime was sufficient to elicit a 20% increase in secreted acid phosphatase activity that is indicative of Pi starvation (Robinson et al., 2012). Moreover, phosphatase activities were identical in wild type and *sgs3-3* plants suggesting that the mutation has no obvious effect on normal responses to Pi starvation.

We screened transgenic lines for cpFLIPPi-80μ, -200μ, -1.6m, -4.8m, -5.3m, and -6.4m and found that only those with K_d values of 4.8 mM and greater showed a significant change in FRET ratio and in each of these cases the ratio increased in response to Pi starvation, consistent with decreased cytosolic Pi concentrations (Fig. 10). Transgenic lines expressing the cpFLIPPi-6.4m sensor showed the largest change in FRET ratio. Moreover, representative FRET images shown in Fig. 10 also suggest that the cytosolic response to Pi deprivation is nearly uniform among root epidermal cells.

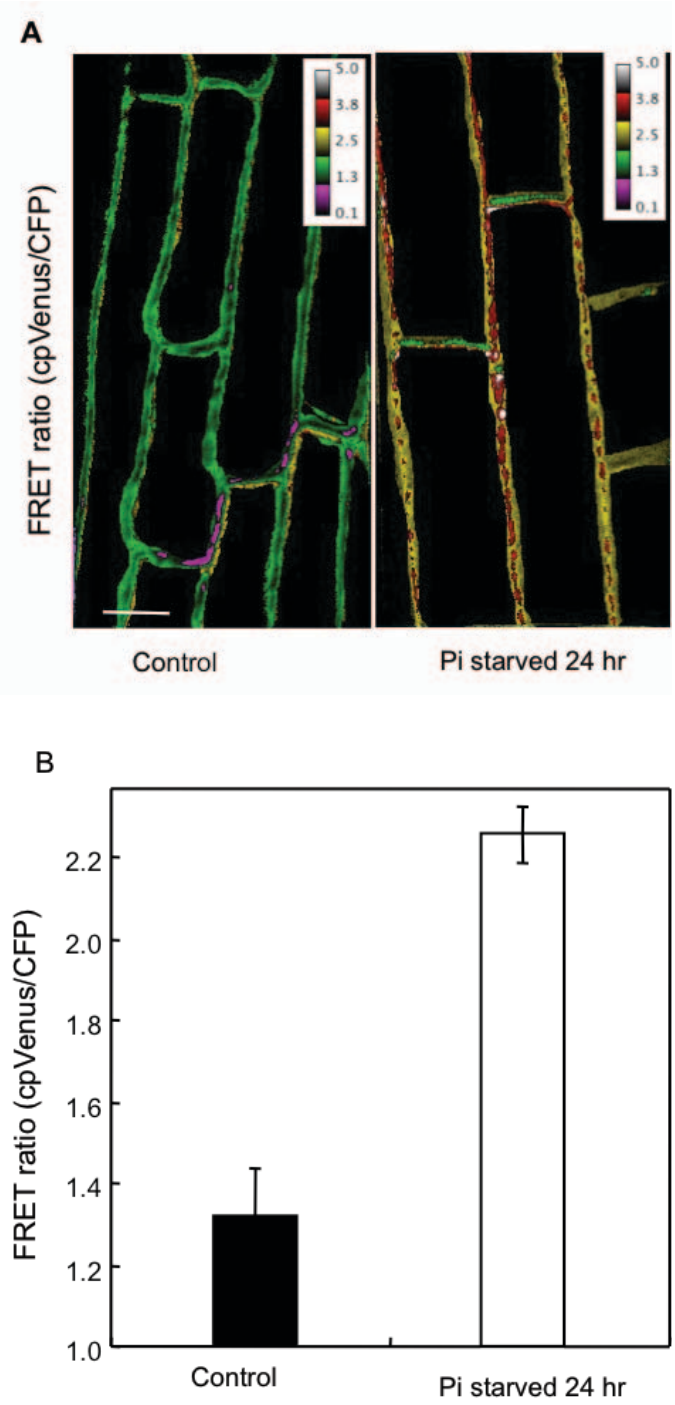

Figure 10. Live imaging of Pi-dependent FRET in root epidermal cells. A, Representative ratio image of cpFLIPPi-6.4m expressed in wild-type plants grown with sufficient Pi (control, left), and after 24 hr Pi starvation (right). The same pseudocolor scale was applied to ratio values for both images. B, The plotted Pi-dependent FRET ratio values are mean ± SE for six independent seedlings.

To test whether FRET ratios in Pi-starved plants could be reset by replenishment with Pi we added 0.5 mM Pi to 24 hour-starved cpFLIPPi-6.4 lines and monitored FRET over time (Fig. 11). No changes were detected when FRET was monitored every 3 seconds for the first few minutes. However, changes in FRET ratios indicative of replenishment were detected after 1 hour and FRET signals were nearly equivalent to the initial "fed" state within 8 hours (Fig. 11). These results strongly indicate that the *in vivo* FRET responses are specific for Pi.

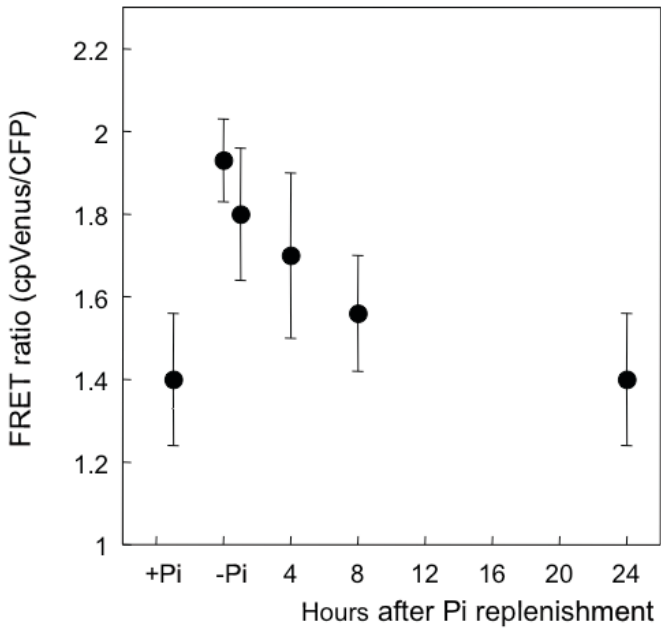

Figure 11. Dynamics of cytosolic Pi replenishment. Seedlings expressing cpFLIPPi-6.4m were grown with a sufficient supply of Pi (0.5 mM, +Pi), starved for Pi for 24 hr (-Pi) then Pi was added to 0.5 mM and FRET ratios were monitored over time. The plotted values are mean ± SE for six independent seedlings. The first time point shown after replenishment is 1 hr.

It was possible that, within limits, the steady state concentration of Pi in the cytosol is a continuum dependent on the magnitude of Pi supply. Alternatively, if other cellular pools buffer cytosolic Pi (Mimura, 1999) then the concentration would be relatively constant until buffering capacity is breached.

To distinguish these possibilities we grew transgenic cpFLIPPi-6.4 lines in hydroponic medium containing 0.5 mM Pi for 5 days then replaced the medium with fresh media containing the same or reduced concentrations of Pi. Plants were grown in the new condition for another 24 hours then imaged in the same final growth medium. As shown in Fig. 12, FRET ratios were nearly constant when plants were supplied with Pi concentrations greater than 25 μM but increased when plants were supplied with lower concentrations.

FRET ratios reached a maximum when plants were supplied with 10 μM Pi, but the values were not significantly different from those measured with plants completely deprived of Pi. These results support the idea that cytosolic Pi is buffered over a broad range of external Pi concentrations, and that this buffering capacity is overwhelmed when Pi supply drops below a critical threshold.

It was formally possible that the changes in cytosolic fluorescent signals we attributed to Pi-dependent FRET were instead due to unrelated changes in the emission of one or both fluorophores. It was not possible to address this issue through analysis of the emission spectrum *in vivo* as was done for our *in vitro* studies. Therefore, we used partial acceptor photobleaching as an alternative approach (Roszik et al., 2008). Evidence for FRET would be revealed by this method if photodestruction of the acceptor

cpVenus resulted in an increase in donor CFP emission due to dequenching of the donor. Moreover, the increase in CFP emission would be proportional to FRET efficiency, which would be dependent on Pi concentration. No consistent change in CFP emission would be expected if sensor responses were unrelated to FRET.

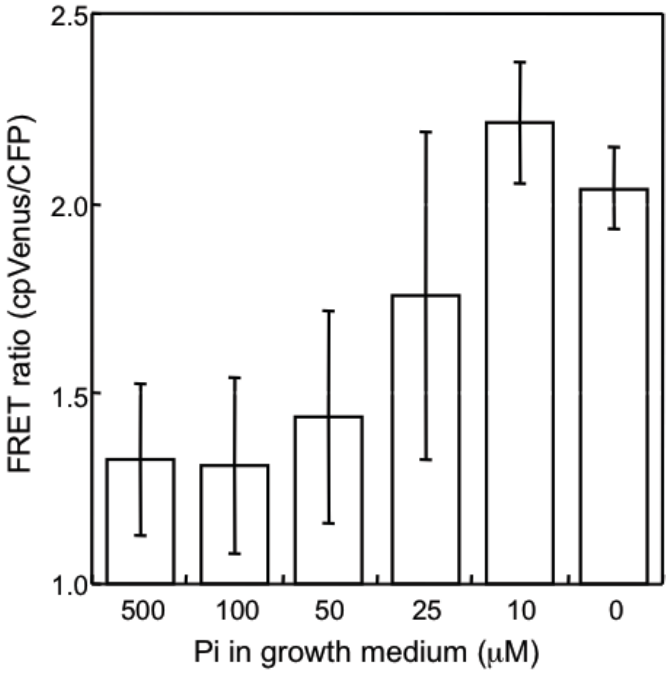

Figure 12. Effect of Pi supply on cytosolic Pi contents of root epidermal cells. Seedlings expressing cpFLIPPi-6.4m were grown with a sufficient supply of Pi (500 μM) then transferred to medium containing the same or less Pi and allowed to equilibrate for 24 hr before imaging. Plotted FRET ratio values are mean ± SE for at least six independent seedlings.

We conducted partial acceptor photobleaching with each of the same plants used to evaluate the effect of different amounts of Pi supply on steady-state levels of Pi in the cytosol (Fig. 12). In each case, CFP emission clearly increased as cpVenus emission diminished, indicating a FRET response (Fig. 13A). FRET efficiencies were calculated from the photobleach responses as described previously (Roszik et al., 2008). The FRET efficiency values calculated for each concentration of supplied Pi directly correlated with the corresponding FRET ratios (Fig. 13B). These results confirmed that the Pi-dependent changes in fluorescent signals we measured were indeed due to FRET and further validated the efficacy of the cpFLIPPi-6.4m sensor for monitoring cytosolic Pi.

Live imaging of steady-state Pi concentrations in root plastids of wild type and a plastidic Pi transport mutant

Nonphotosynthetic plastids import ATP from the cytosol in stoichiometric exchange for stromal ADP (Reiser et al., 2004; Reinhold et al., 2007). A consequence of the unbalanced phosphate moieties associated with this exchange is that Pi would accumulate to deleterious levels if not balanced by export. We proposed previously that the plastidic Pi transporter PHT4;2 confers this export activity in root plastids (Irigoyen et al., 2011). Transport activities measured with root plastids isolated from wild type and a *pht4;2* mutant support this idea. However, the mutation also reduced Pi import.

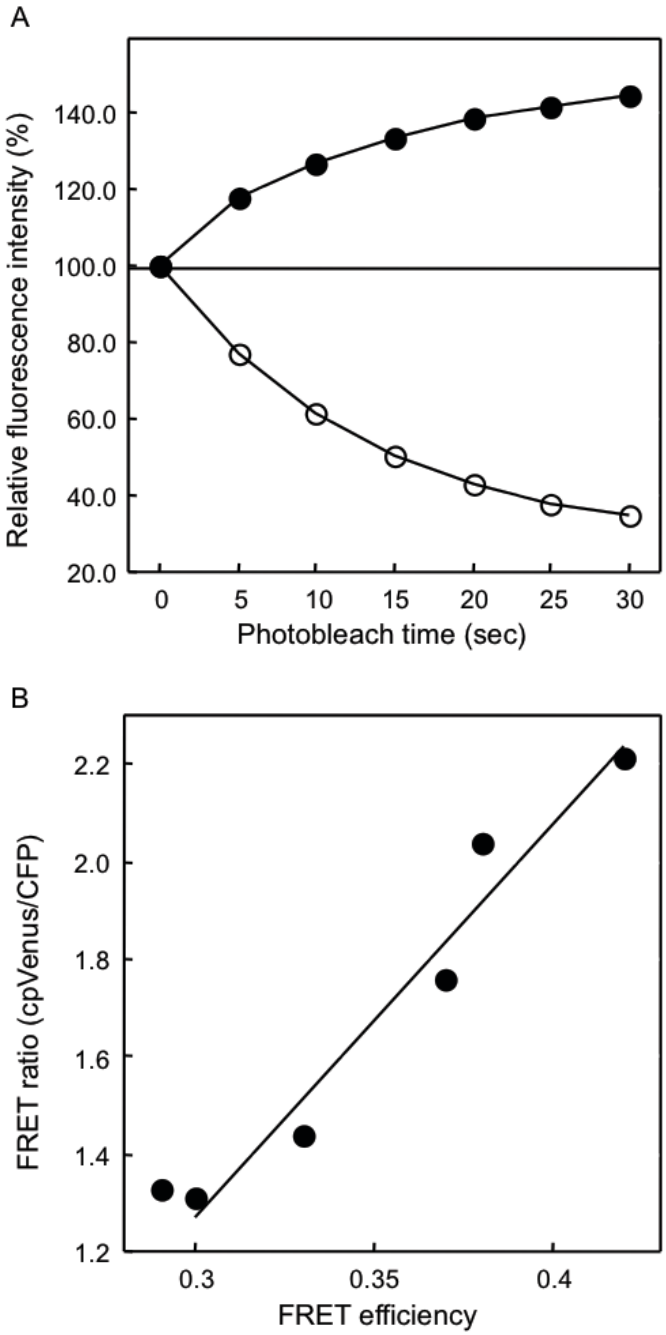

Figure 13. Partial acceptor photobleaching of cytosolic cpFLIPPi-6.4m reveals a direct correlation between Pi-dependent FRET efficiency and FRET ratios. A, Representative photobleaching results for one plant showing that increased photodestruction of cpVenus (open circles) results in increased CFP emission (filled circles). These responses were used to calculate FRET efficiencies. B, Plot of FRET ratios from Fig. 12 vs. FRET efficiencies for the same concentrations of supplied Pi.

It was possible that the import activity simply reflected the reversibility of the transport process especially since maintenance of relevant electrochemical gradients cannot be assured with isolated organelles. Alternatively, PHT4;2 may have an undefined role in Pi import.

To directly assess the role of PHT4;2 in plastidic Pi homeostasis within the context of an intact plant we introduced the cpFLIPPi-6.4m sensor into the *pht4;2* background then compared FRET signals in this line to those of the same sensor in wild type. Plants were grown for 5 days in medium containing 0.5 mM Pi to establish uniform growth then imaged in the same medium.

As shown in Figs. 14-15, FRET signals were significantly lower in the mutant, consistent with hyperaccumulation of Pi. This result strongly supports the idea that the primary role of PHT4;2 is Pi export. In addition, overlay of the FRET ratio images with DIC images to distinguish individual cells revealed that there is little variation in the amounts of Pi accumulated in plastids within the same cell and in different epidermal cells (Fig. 14).

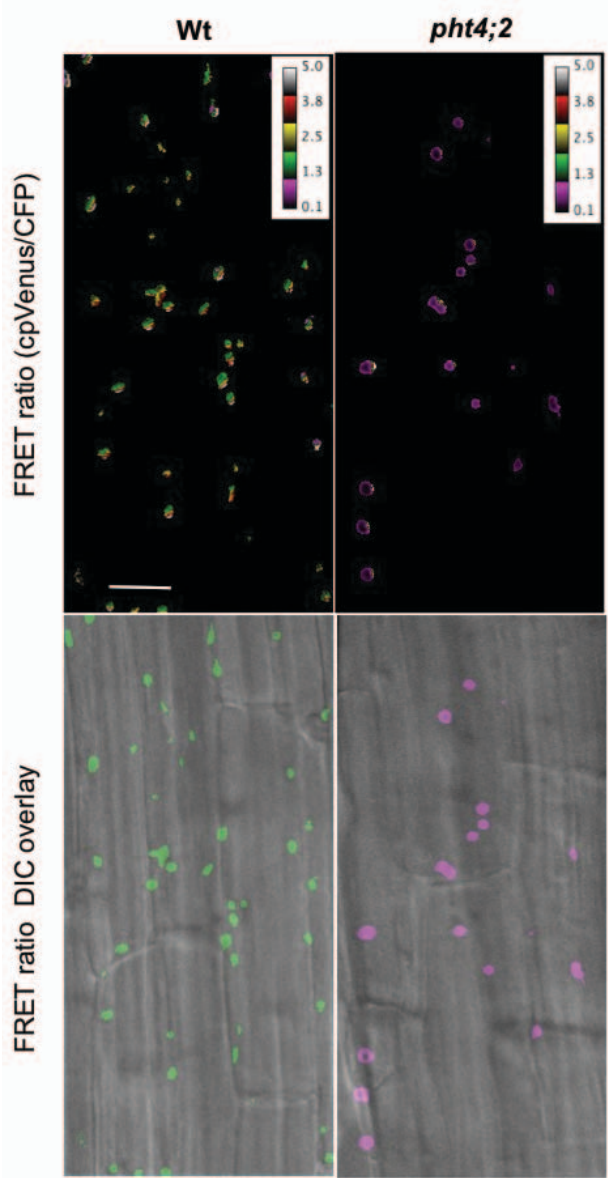

Figure 14. Live imaging of Pi-dependent FRET in plastids of root epidermal cells. The top panels are representative ratio images of cpFLIPPi-6.4m expressed in wild-type and *pht4;2* plants grown with sufficient Pi. The same pseudocolor scale was applied to each image. The bottom panels are DIC overlays of the same regions shown in the top panels to distinguish cell boundaries. Size bar, 5 μm.

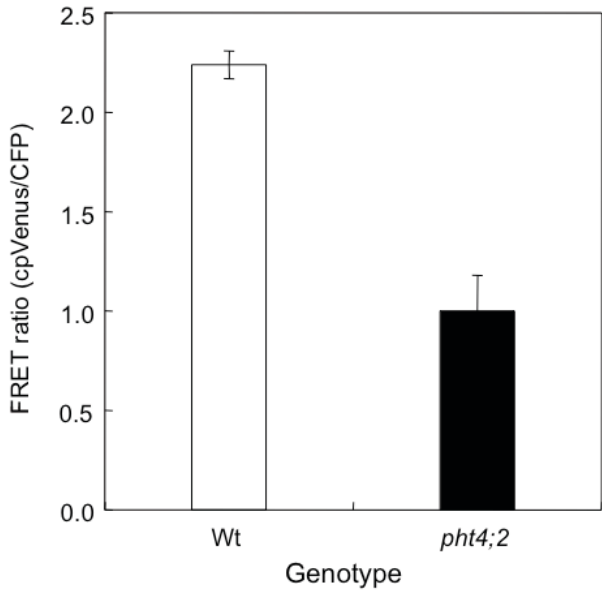

Figure 15. Comparison of Pi-dependent FRET in root plastids of wild-type and *pht4;2* plants. FRET ratios were determined for plastid-targeted cpFLIPPi-6.4m in wild-type and *pht4;2* plants grown with sufficient Pi. The values plotted are mean ± SE for six independent seedlings.

Discussion

To monitor Pi levels in live plants with cellular and subcellular resolution we optimized a FRET-based Pi sensor (FLIPPi) developed previously (Gu et al., 2006). Two key attributes that required optimization were signal gain and binding affinity. We substituted the eYFP component of a FLIPPi sensor with a circularly permuted form of Venus and confirmed that this modification provides nearly 150% greater FRET signal gain (Fig. 3). We used a mutagenesis strategy to alter binding affinity of this circular permuted FLIPPi (cpFLIPPi). This strategy involved a novel use of statistical coupling

analysis (SCA) (Lockless, 1999; Socolich et al., 2005) as a means to enhance the efficiency of our mutant screen. The premise of SCA is that coupling represents an evolutionary constraint for structural or functional properties, e.g., ligand binding, protein-protein interactions and allosteric sites. We conducted SCA with a set of 1020 conserved Pi binding proteins and identified a 6 amino acid region that contained coupled residues that also map near the predicted Pi binding site. By limiting our mutagenesis to alter only this 6 amino acid region rather than exploring the entire 340 amino acids of the Pi binding protein included in the cpFLIPPi sensor, we reduced the scope of mutagenesis numerically and also greatly biased our screen for those likely to alter Pi binding properties. Indeed, of the nearly 600 mutants screened, less than 1% resembled the parent sensor. Approximately 80% of the mutants exhibited Pi-dependent FRET, but with altered affinity. The remaining ca. 20% of the mutant population were wither unresponsive to Pi or had fluorescence signals too low to accurately assess binding responses.

We purified and analyzed Pi-dependent FRET for eight cpFLIPPi sensors using an *in vitro* binding assay designed to approximate *in vivo* conditions (Messerli and Robinson, 1998; Feijó et al., 1999). These sensors proved to be highly specific for Pi and the K_d values for Pi binding ranged from 0.08 to 11 mM, which spans the predicted physiological range of 2.5 to 10 mM for the cytosol and plastid stroma (Rebeille et al., 1984; Stitt et al., 1988; Lee and Ratcliffe, 1993; Copeland and Zammit, 1994; Gout et al., 2011). Although *in vivo* binding affinities may differ from those determined *in vitro*, the large (>100-fold) concentration range collectively probed by these cpFLIPPi sensors

was sufficient to monitor relative changes in the Pi contents of cytosol and plastid stroma of Arabidopsis root cells. The modest sensitivity to pH we observed for the sensors could be attributed entirely to specificity for the monobasic form of Pi. Nevertheless, the differences indicate that *in vivo* comparisons should be restricted to the same cellular compartment.

FRET sensors can be subject to gene silencing when expressed in plants (Deuschle et al., 2006). We also detected weak or unstable fluorescent signals in transgenic plants, suggestive of gene silencing. To minimize this problem we used the silencing deficient *sgs3-13* mutant (Deuschle et al., 2006; Yang et al., 2010) as a base-line host for our studies. Secreted acid phosphatase activities measured in Pi-sufficient and Pi-starved *sgs3-13* seedlings matched those of wild-type seedlings grown under the same conditions suggesting that this mutation has no significant effect on normal responses to Pi starvation.

Pi deprivation for 24 hours was sufficient to elicit a significant change in FRET indicative of decreased cytosolic Pi. This response was detected only for sensors with *in vitro*-derived K_d values of 4.8 mM or greater, which suggests that sensors with higher affinity for Pi remained effectively saturated under this relatively mild starvation regime. Transgenic lines with the cpFLIPPi-6.4m sensor yielded the largest change in FRET upon Pi deprivation, which may reflect an optimal pairing of the binding affinity of this sensor with cytosolic Pi concentration.

Two lines of evidence indicate that the changes in FRET we measured represent genuine Pi-dependent responses. First, changes in FRET elicited by Pi deprivation were

completely reversed by Pi replenishment. Second, acceptor photobleaching experiments revealed that changes in FRET ratios directly correlate to Pi-dependent FRET efficiencies. Consequently, we conclude that cpFLIPPi sensors report changes in cytosolic Pi concentration with high specificity. Moreover, our results suggest that the concentration of Pi in the cytosol is relatively constant despite large differences in the amount of Pi supplied in the growth medium. However, this buffering of cytosolic Pi concentration can be overwhelmed when Pi supply falls below a critical threshold. For our assay conditions, this threshold is 25 μM.

The PHT4;2 phosphate transporter is located in root plastids (Guo et al, 2008a; Guo et al, 2008b). We proposed that the *in vivo* function of this transporter is to export Pi from root plastids, which would be necessary to avoid deleterious accumulation that would otherwise arise due to the imbalance of phosphate moieties associated with uptake of ATP in exchange for ADP (Neuhaus and Maass, 1996; Neuhaus and Emes, 2000). Transport assays conducted with isolated root plastids agreed with this hypothesis, but also revealed an import activity (Irigoyen et al., 2011). It was not clear whether the import activity represented transport reversibility under our assay conditions or reflected a novel *in vivo* activity. FRET measurements for a plastid-targeted cpFLIPPi-6.4m sensor expressed in wild-type and *pht4;2* seedlings indicated that *pht4;2* root plastids hyperaccumulate Pi, thus confirming that the primary role for PHT4;2 *in vivo* is Pi export. More applications of the cpFLIPPi sensors will be discussed in Chapter IV.

Materials and Methods

Plasmids

We obtained FLIPPi plasmid clones pRSET FLIPPi-200μ and pRSET FLIPPi-30m (Gu et al., 2006) from Addgene (www.Addgene.com). To replace the eYFP coding region of pRSET FLIPPi-200μ with a circularly permuted version of Venus, we first amplified the cp173 coding region from the YC3.60 Ca^{2+} sensor (Nagai et al., 2004). We then used PCR and the In-Fusion (Clontech) cloning kit to introduce this sequence into the same region occupied by the eYFP coding sequence in the pRSET FLIPPi-200μ plasmid to generate pRSET cpFLIPPi-200μ.

For cpFLIPPi sensor expression in plants, a 2455 bp Hind III-BamHI segment of the desired pRSET cpFLIPPi clone was ligated into pCN-UBQ10, a modified pCAMBIA3300 plasmid. The modifications included insertion of the Arabidopsis *UBQ10* promoter (Norris et al., 1993) to direct expression of the sensor gene and replacement of the *35S* promoter located upstream of the phosphinothricin resistance gene with the *Nos* promoter of pBI121. A plastid-targeted variant of each clone was constructed by inserting a 237 bp fragment encoding the 79 amino acid RbcS chloroplast transit peptide (Lee et al., 2006) in frame at the 5' end of the sensor gene.

Construction of a cpFLIPPi affinity mutant library

We used statistical coupling analysis (SCA) (Lockless, 1999; Socolich et al., 2005) as a guide to generate a sensor mutant library biased for altered affinity. Sequences were collected from the nr database (as of 5/5/2010) using PSI-BLAST

(Altschul et al., 1997). The *Escherichia coli* PiBP protein (GI:157829674) was used as the query for five iterations of PSI-BLAST. Sequences with an e-score<1e-10 were aligned using MUSCLE (Edgar, 2004). Identical sequences were eliminated and the alignment of the remaining 1020 sequences was used for SCA. SCA was performed as previously described (Lockless, 1999; Socolich et al., 2005) to identify the set of positions that co-evolve with one another. Two rounds of hierarchical clustering were performed to yield a self-consistent set of positions that statistically co-vary with each other. PiBPs have one self-consistent cluster consisting of 43 amino acids (13% of protein), which is mapped onto the structure of the *E. coli* PiBP using PyMol (Fig. 6).

A stretch of six amino acids (positions 18-23) within the 43 amino acid cluster was identified as a high-value mutational target based on the following observations: 1) four of the positions (#18, 19, 21 and 23) co-evolve with one another, 2) one position (#20) is highly conserved, 3) they are located near to the Pi binding site, and 4) the positions could be simultaneously mutated with one set of oligonucleotides. The mutagenesis oligonucleotides were designed such that each position was mutated to the three most frequently observed amino acids in the alignment that are found in at least 9% of sequences. In practice, this means that more than the desired amino acids are possible at some positions since the nucleotides required to encoded the target amino acids can also encode other amino acids. For example, alanine (GCT codon), aspartate (GAT codon) and serine (TCT codon) are needed at position 19, but the nucleotides required in the oligonucleotide at each position can also encode for tyrosine (TAT codon).

The pRSET cpFLIPPi-200μ plasmid was used as template for PCR mutagenesis.

The mutagenesis oligonucleotides 5'-ccaaaccgtgcaaatctccRBCKMTgggcKCGDMCDYCgcggctcctttgctgcaacgttg and 5'-gttgcagcaaaggagccgcGRHGKHCGMgccAKMGVYggagatttgcacggtttgggctt introduce ca. 1728 possible amino acid combinations for the six amino acid (positions 18-23) target region. The amplicon population was restriction digested then ligated into pRSET cpFLIPPi-200μ, replacing the original sequence. A portion of this mixed ligation product was introduced into *E. coli* DH5α cells and >10,000 colonies were pooled for bulk plasmid isolation. The isolated plasmids collectively represent the affinity mutant library.

cpFLIPPi affinity mutant screen

Portions (0.1 ng) of the sensor affinity mutant plasmid library were introduced into *E. coli* BL21 (DE3) cells. The pRSET cpFLIPPi-200μ plasmid served as a positive control and pUC19 served as a negative control for each transformation and subsequent screen. Individual colonies were transferred to a 96-well plate containing 45 μl LB medium in each well and mixed thoroughly. Twenty μl aliquots were transferred to duplicate 96-well deep well plates containing 1.5 ml LB medium then covered with a gas-permeable seal. Plates were shaken at 300 rpm for 16 hours at 25°C. Glycerol stocks were prepared from 0.1 ml aliquots of each culture in a separate 96-well plate and stored ay -80°C. The growth plates were centrifuged for 30 min at 2800 rpm to pellet cells then the supernatant was removed by vacuum aspiration. Cell pellets were washed twice with 20 mM Tris-HCl, pH 7.5 then frozen at -20°C. To lyse cells, 0.35ml lysis solution (1x

BugBuster (Novagen), 20 mM Tris-HCl pH 7.5, 150 mM K-gluconate, 3 μl Lysonase/ml) was added to each well, mixed thoroughly then incubated at room temp for 20 min with mixing every 5 minutes. Plates were then centrifuged for 10 min at 2800 rpm, 20°C to remove cell debris.

Fluorescence assays were conducted with lysates in 96-well black plates. We transferred 20 μl aliquots of each lysate to eight wells containing 200 μl pseudocytosol medium (100 mM K-gluconate, 30 mM NaCl, 25 mM MES, 25 mM HEPES, 40% sucrose, 1 mg/ml BSA, pH 7.5) (Messerli and Robinson, 1998; Feijó et al., 1999) and varied amounts of Pi (0 to 30 mM). Fluorescence was measured using a microplate reader (Synergy HT) with excitation 420/27 nm and emission 485/20 and 540/25 nm. Fluorescence from direct excitation of cpVenus (500/20 nm) was also monitored with emission at 540/25 nm. The K_d value for each sensor lysate was estimated by fitting data to a single-site binding isotherm as described (Gu et al., 2006).

In vitro characterization of cpFLIPPi proteins

Selected cpFLIPPi mutant clones were re-introduced into *E. coli* BL21 (DE3) cells, and single colonies were cultured in 100 ml medium then harvested and lysed essentially as described above for the mutant screen. The expressed sensor proteins were purified from cell lysates using His-affinity chromatography with elution in 20 mM Tris-HCl pH 7.5, 150 mM K-gluconate, 400 mM imidazole. The eluent was dialyzed overnight at 4°C against 20 mM Tris-HCl pH 7.5 then transferred to a new tube and stored at 4°C. The purified sensors could be stored for at least one month without

measurable change in fluorescence or binding properties. K_d values were determined as described above for the mutant screen, but twelve Pi concentrations were used to generate binding curves. Assays for binding affinity, specificity and pH sensitivity were all conducted with at least three independent protein preparations.

Generation of transgenic Arabidopsis plants

Sensor transgenes were introduced into Arabidopsis *sgs3-13* plants by floral dip transformation (Clough and Bent, 1998)

Subcellular localization of sensor proteins

Protoplasts were prepared as described (Yoo et al., 2007) from leaves of 4-week-old transgenic plants expressing cpFLIPPi sensors engineered with and without an N-terminal RbcS chloroplast transit peptide. Protoplasts were imaged with a BioRad ES confocal laser scanning microscope equipped with a 63x (numerical aperture, 1.2) water-immersion objective (515 nm excitation, 540 nm emission for direct excitation of the cpVenus sensor component, and 488 nm excitation, 680 nm emission for chlorophyll autofluorescence.

Live imaging of sensors in plants

Transgenic plants were grown in individual wells of 96-well plates with 300 µl of hydroponic mediu in each well. This medium contained 1% sucrose and unless indicated otherwise, also contained 500 µM Pi. The plates were incubated in a growth

chamber (60% relative humidity, 21°C, 90 μmol m^{-2} s^{-1} light intensity, 14 hour photoperiod). After 5 days the seedlings were either imaged or transferred to fresh medium as indicated for an additional 24 hours before imaging. For imaging, seedlings were placed in a custom-made chamber (http://microscopy.tamu.edu/lab-protocols/light-microscopy-protocols.html) containing the same growth medium. Seedlings were covered with a small square of nylon mesh then held in place with a glass weight. A similar procedure was described recently (Kruger et al, 2013). Seedlings were analyzed for FRET using an inverted Olympus IX81 laser spinning disk confocal microscope equipped with an Andor Opti-splitter to allow simultaneous dual emission. Root epidermal cells were viewed with a 40x oil-immersion objective (445 nm excitation for CFP and 483/32 and 542/27 nm emission wavelengths for CFP and FRET-derived cpVenus, respectively. Laser intensity and exposure settings were kept constant. For acceptor photobleaching experiments, a 515 nm excitation laser was used with maximum laser intensity. Untransformed seedlings and transgenic seedlings expressing CFP alone and cpVenus alone were imaged each day to allow correction for background fluorescence and spectral bleedthrough.

All image analyses were done using ImageJ software. For ratiometric analysis (sensitized emission), images were background subtracted and corrected for spectral bleedthrough. For analysis of cytosol-localized sensors, intensity values for CFP and cpVenus were measured for selected regions of interests (ROIs). For analysis of plastid-localized sensors, a uniform threshold was applied to the CFP and FRET-cpVenus images, and mean intensity values above the threshold were used to calculate FRET

ratios. FRET efficiencies (E-values) were calculated from partial acceptor photobleaching images as described (Roszik et al., 2008).

CHAPTER III

ANALYSIS OF ARABIDOPSIS CHLOROPLAST PHOSPHATE TRANSPORTER MUTANTS

Introduction

Plastids are specialized organelles present in all plant cells. These diverse organelles are the sites of a wide range of essential biological processes like photosynthesis, nitrogen and sulfur assimilation (Lopez-Juez and Pyke, 2005), as well as the manufacture and storage of amino acids, starch, fatty acids and secondary metabolites (Neuhaus and Emes, 2000). Tightly regulated exchange of metabolites between the plastid stroma and cytosol is necessary for coordinating these vital functions. The transport of Pi between these compartments is especially important, as it is involved in virtually all metabolic pathways and has a strong effect on photosynthesis and carbon partitioning (Flügge and Heldt, 1984; Flügge, 1999). The focus of this chapter is to investigate Pi homeostasis in the chloroplast to with the goal of increasing our understanding of plant growth and metabolism.

Plastids can be categorized as autotrophic like chloroplasts (photosynthesis) and heterotrophic like elaioplasts (oil storage), amyloplasts (starch storage), chromoplasts (synthesis of chromoplast) (Whatley, 1978). Like all plastids, chloroplasts have a double membrane envelope, and the inner membrane serves as a permeability barrier. The inner membrane also houses several transporter proteins that mediate Pi exchange between cytosol and stroma. Plant Pi transporters are integral

membrane proteins comprising 12 membrane spanning regions, divided into two groups of six by a large hydrophilic charged region in between them. Pi transporters might have originated by tandem intragenic duplication, a proposal supported by its conserved motifs and sequences in the two halves of the protein. Plastidic Pi transport is generally attributed to the members of the plastidic phosphate translocator (pPT) family, all of which are antiporters that catalyze the exchange of Pi for phosphorylated C3, C5 or C6 carbon compounds across the inner envelope membrane (Kammerer et al., 1998; Flügge, 1999; Neuhaus and Emes, 2000; Knappe et al., 2003; Weber, 2004). The details of this transporter family were discussed in chapter 1.

Chloroplasts rely on the import of Pi from the cytosol to support ATP synthesis via photophosphorylation, which in turn, fuels the Calvin cycle. This Pi import activity is generally attributed to TPT, the most well studied member of pPT family. The partitioning of triose-P toward sucrose biosynthesis in the cytosol or transitory starch in the stroma also involves TPT and is controlled, at least in part, by the concentrations of Pi in the cytosol and stroma. When exported to the cytosol, triose-P is used for the synthesis of sucrose, which is the major form of carbon distributed to heterotrophic tissues. Pi released from organic compounds during sucrose synthesis is available for return to the chloroplast to replenish ATP. As sucrose biosynthesis slows during the day due to low sink demand, cytosolic P remains trapped in organic compounds and cytosolic Pi levels decline, limiting further counter exchange with triose-P. As a result, stromal Pi levels decrease, and triose-P is redirected to starch biosynthesis, which also recycles Pi in the stroma to support continued photosynthesis. Starch synthesis is

favored when stromal Pi levels are low because Pi is an allosteric inhibitor of ADP-glucose phosphoylase (ADGPase), the first committed step of starch synthesis (Sheu-Hwa et al., 1975; Preiss, 1982; Ballicora et al., 2004)

Despite the importance of TPT for both chloroplast Pi import and carbon partitioning, *tpt* mutants do not show any growth defect under normal growth conditions. These plants do exhibit increased starch synthesis and turnover rates to compensate for the defect in carbon allocation (Barnes et al., 1994; Schneider et al., 2002; Walters et al., 2004), which suggests that compensatory or redundant mechanisms also exist for the coupled defect in Pi import. Genome sequence mining has revealed additional plastidic Pi transporters that are unrelated to members of the pPT family, and such transport has been termed unidirectional (Neuhaus and Maass, 1996; Neuhaus and Wagner, 2000). Pi transport by these proteins does not appear to be coupled to carbon transport and may reflect passive uniport or active, symport mechanisms in the chloroplast inner membrane. To date, six unidirectional plastidic Pi transporter candidates have been identified in Arabidopsis. These include PHT2;1 (Daram et al., 1999; Versaw and Harrison, 2002) and five members of the PHT4 family (Table I). Although PHT2;1 and PHT4;4 are both predicted to have 12 membrane-spanning domains, these proteins are phylogenetically unrelated. PHT2;1 shares similarity to mammalian type III Na^+/Pi symporters, whereas PHT4;4 shares similarity to the structurally distinct mammalian type I Na^+/Pi symporters. PHT2;1 and PHT4;4 are both located in the chloroplast inner membrane (Ferro et al., 2002; Versaw and Harrison, 2002; Guo et al., 2008a), and functional studies in yeast confirmed that these proteins

mediate Pi transport (Guo et al., 2008a). Transport activities in yeast are sensitive to pH and to protonophores suggesting that these transporters are dependent on a pH gradient and/or membrane potential. We used reverse genetics approaches to characterize two candidates for unidirectional Pi transport in plastids, PHT2;1 and PHT4;4 (Versaw and Harrison, 2002; Guo et al., 2008a). A model of plastid transport mechanisms is shown in Fig 16.

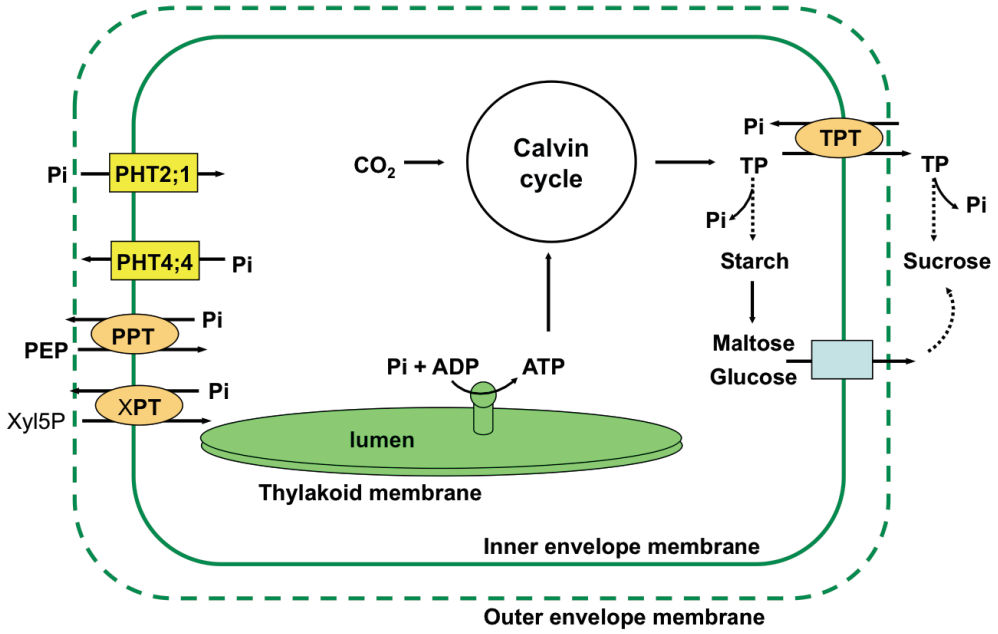

Figure 16. Model for chloroplast phosphate transport. TP, triose-P; Xyl5P, Xylulose 5-P; PEP, Phosphoenolpyruvate. Pi transporters are located in the inner membrane of the chloroplast.

My work focused on understanding the roles of PHT4;4 and PHT2;1 in the chloroplast. These proteins are localized in the inner envelope of chloroplasts, but the physiological relevance of unidirectional Pi transport in the chloroplast inner envelope is unknown. To investigate the physiological roles of unidirectional Pi transport across the chloroplast inner envelope I isolated null mutants for PHT2;1 and PHT4;4 transporters. These mutants exhibit growth defects under defined conditions, which underscored the importance of the affected transporters. Surprisingly, *pht4;4* mutants accumulated greater biomass than wild type through increased cell proliferation in leaves.

I hypothesized that unidirectional Pi transporters provide fine-tuning of Pi levels in multiple plastid types and compartments, and that this control has broad implications for plant metabolism, growth and development.

Results

Mutant isolation and molecular characterization

As one approach to determine the physiological roles of PHT2;1 and PHT4;4, I chose to characterize mutants that lack these proteins. I also wanted to include in my studies a mutant that lacks TPT to eliminate this source of Pi transport activity from the different genetic backgrounds. A *pht2;1* null mutant was isolated and characterized previously (Versaw and Harrison, 2002). A *tpt* mutant was isolated previously by a colleague in lab, and it is null based on the absence of *TPT* transcripts.

I isolated two independent transposon insertion lines for *PHT4;4* from the Cold

Spring Harbor collection, and these were named *pht4;4-1* and *pht4;4-2*. The structure of the *PHT4;4* locus for these alleles was deduced from PCR, Southern blots and the sequence of PCR products, and is depicted in Fig 17. *pht4;4-1* had an insertion in the first exon and *pht4;4-2* has an insertion in the first intron. Both insertions also resulted in small deletions, 8 bp for allele 1 and 18 bp for allele 2.

To test whether these mutants lacked *PHT4;4* transcripts, which would be indicative of null mutations, I conducted RT-PCR using primers that anneal downstream as well as flanking the insertion sites. No *PHT4;4* transcripts were detected for *pht4;4-1* using primers downstream or flanking the insertion site (Fig.17). Similarly, no transcripts were detected for *pht4;4-2* using primers that flank the insertion. However, a transcript was detected with primers that anneal downstream of the insertion (Fig.17). RT-PCR using a transposon-specific primer and a *PHT4;4*-specific primer followed by sequencing of the amplified product confirmed that the transcript initiates within the transposon.

If this transcript were translated, the protein would lack the N-terminal plastid targeting sequence. Moreover, phenotypic analysis (described below) showed that both alleles have the same phenotype. Therefore, I conclude that both alleles are null. Southern blot analysis showed that both of the homozygous mutant lines contained a single transposon insertion (Fig. 18).

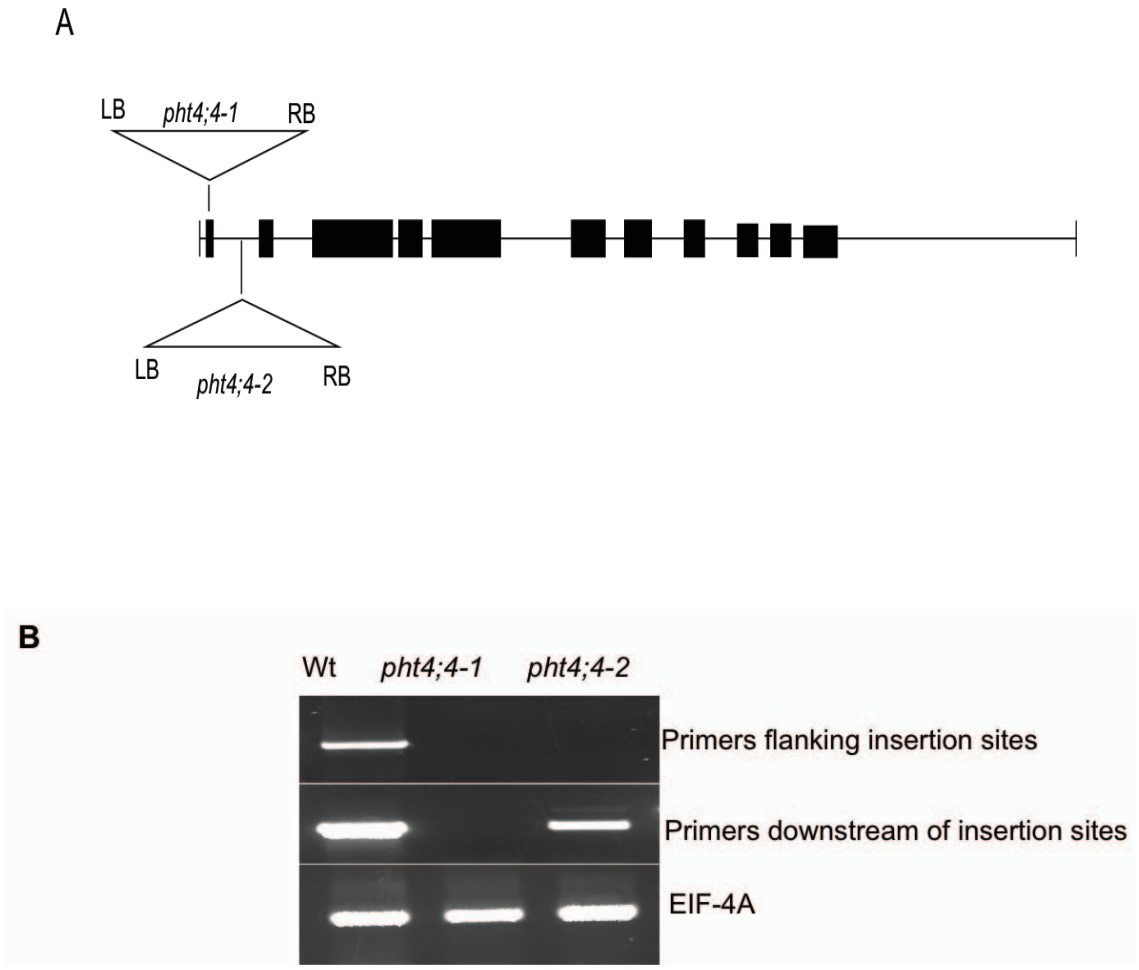

Figure 17. Location of transposon sites for *pht4;4* mutations. A, Transposon insertion sites were determined by PCR and sequencing of junction amplicons. Small arrows represent the primers used for PCR. Black boxes represent exons and lines represent introns.
B, RT-PCR analysis of *pht4;4-1* and *pht4;4-2* mutants. Primers anneal to sites flanking or downstream of the insertion sites as indicated.

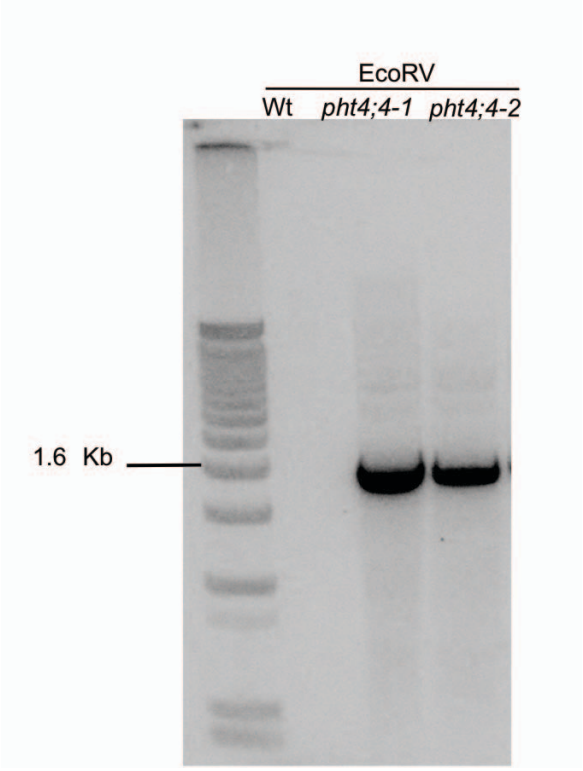

Figure 18. *pht4;4-1* and *pht4;4-2* mutants both carry a single transposon insertion. DNA gel blot was probed with the *Gus* gene. *Eco*RV cuts within the probed region and flanking sequences, yielding 1452 bp for *pht4;4-1* and 1552 bp for *pht4;4-2*.

pht4;4 leaves are larger than wild type when plants are grown under low-light conditions

Like *tpt*, *pht4;4-1* and *pht4;4-2* do not show any significant phenotype under standard growth conditions. However, when plants were grown with low light intensity (60 µmol m^{-2} s^{-1}), *pht4;4* mutants were 35% larger than the wild type in terms of area and biomass (Fig. 19). The *pht4;4-1* mutation co-segregates with the size phenotype (Fig. 20), consistent with the idea that the mutation is responsible for the phenotype. Also, disruption of *PHT4;4* appears to be dominant (Fig. 20). Given that the mutation is null, I hypothesize that dominance reflects a dosage effect, i.e., haploinsufficiency.

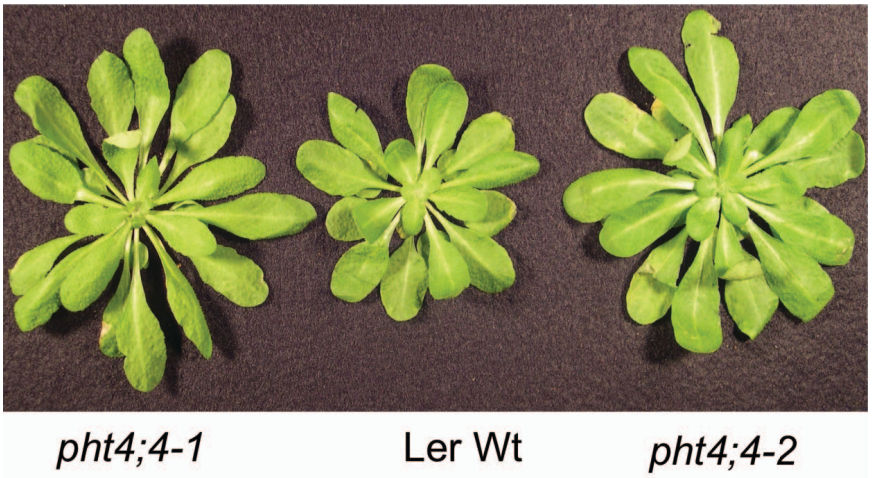

Figure 19. Size phenotype of *pht4;4* mutants. Plants were grown for 9 weeks with 8 hr photoperiod, light intensity 60 µmol m^{-2} s^{-1}. n=10.

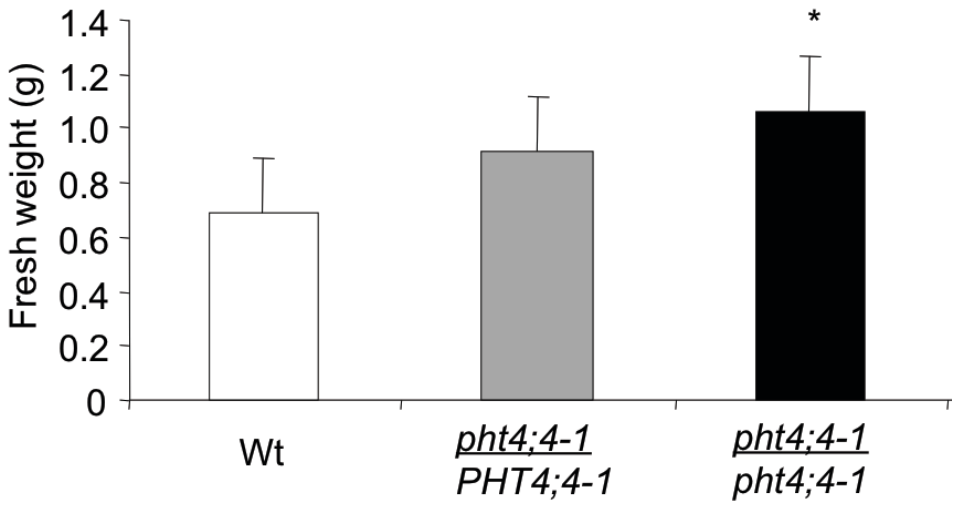

Figure 20. Segregation analysis of *pht4;4-1*. F2 plants were grown for 9 weeks with 8 hr photoperiod, light intensity 60 µmol m^{-2} s^{-1}(n= 36). Error bars indicate standard error. Difference between all three classes is significant ($p < 0.005$).

pht4;4-1 leaves have more cells than wild type

The large-size phenotype of *pht4;4* could result from more cells, larger cells, or a combination of these changes. To distinguish between these possibilities, I examined epidermal and mesophyll cells in leaf 9 of 7-week-old mutant and wild-type plants (Fig. 21). I found that *pht4;4-1* has 27% more cells than the wild type (Table III). The basis for increased cell proliferation is unknown, but a similar phenotype has also been observed for another PHT4 mutant, *pht4;2*, and this is being investigated by a colleague in the lab.

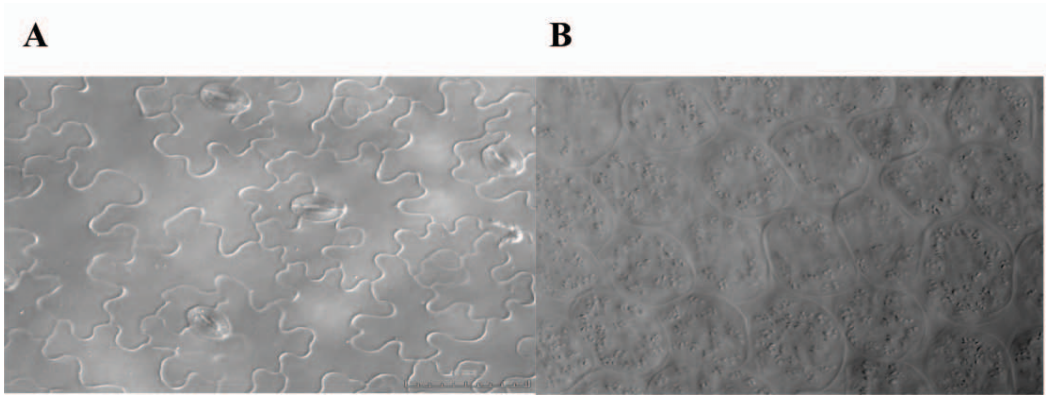

Figure 21. DIC image of *pht4;4* leaves. A, Abaxial epidermal cells of *pht4;4-1*. B, Abaxial mesophyll cells of *pht4;4-1*.

Table III. Rosette and cell sizes at the end of the vegetative growth stage

	Wild type	*pht4;4-1*	*pht4;4-2*
Rosette area (cm^2)	46.4 ± 1.5	63.6 ± 1.9*	69.4 ± 1.7*
Rosette FW (g)	2.15 ± 0.21	2.65 ± 0.10*	2.92 ± 0.09*
Rosette DW (g)	0.22 ± 0.01	0.26 ± 0.01*	0.27 ± 0.01*
Leaf 9 epidermal cell size (μm^2)	1430 ± 80	1470 ± 110	1450 ± 90
Leaf 9 epidermal cell number	266,700 ± 16,900	322,000 ± 25,400*	324,800 ± 20,400*
Leaf 9 mesophyll cell size (μm^2)	1940 ± 110	1910 ± 130	1990 ± 85
Leaf 9 area (cm^2)	3.8 ± 0.1	4.7 ± 0.1*	4.7 ± 0.1*

Plants were grown for nine weeks. Cell areas are calculated from three regions within the ninth rosette leaf. Values are means ± SE (n=10). * Significantly different from the wild type ($p < 0.05$, Students *t* test).

pht2;1 leaves are smaller than wild type

If PHT4;4 and PHT2;1 have redundant functions, then *pht2;1* mutants might also exhibit a large-size phenotype similar to that of *pht4;4* mutants. However, *pht2;1* was smaller than wild type (Fig. 22). This opposite growth phenotype suggests that PHT4;4 and PHT2;1 have distinct roles and may catalyze Pi transport across the chloroplast inner membrane in opposite directions. Interestingly, *tpt* was grown under similar low-light conditions, but its growth was indistinguishable from wild type.

	Fresh Wt (mg)	Dry Wt (mg)
Wild type	730 ± 30	62 ± 3
pht2;1	540 ± 60	43 ± 5

Figure 22. Size phenotype of *pht2;1*. Plants were grown for 9 weeks with 8 hr photoperiod, 60 µmol m^{-2} s^{-1} light intensity. n=10.

pht2;1 and *pht4;4* mutants have opposite starch accumulation phenotypes

Starch synthesis is repressed by high stromal Pi concentration whereas synthesis is enhanced by low concentration. If PHT2;1 and PHT4;4 transport Pi in opposite directions, the mutants might then also show corresponding defects in starch accumulation. To test this hypothesis, leaf starch levels were measured in wild type, *pht2;1* and *pht4;4* plants. *pht4;4* starch levels were 25% less than wild type, whereas *pht2;1* starch levels were 40% greater than wild type (Fig. 23).

Based on growth and starch phenotypes, I propose a model for chloroplast Pi transporter activities (Fig. 15) in which PHT2;1 contributes to Pi import (defect results in low stromal Pi level that stimulates starch synthesis) and PHT4;4 contributes to Pi export (defect results in high stromal Pi level that limits starch synthesis).

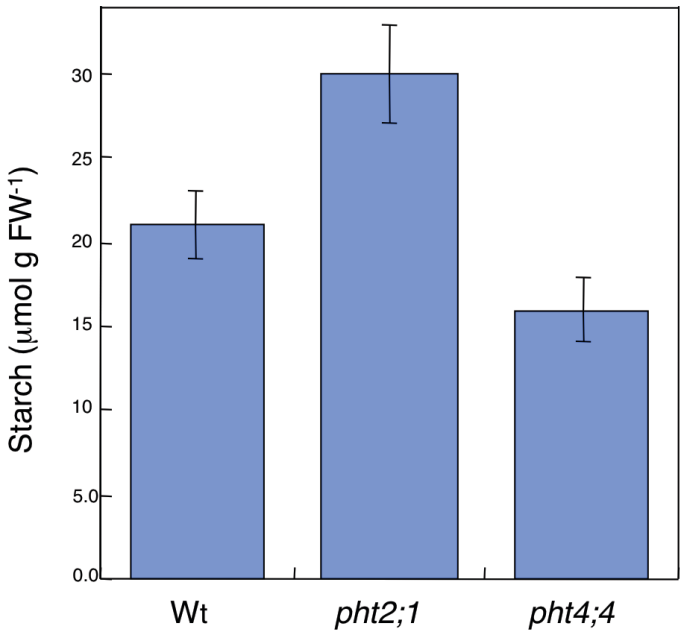

Figure 23. Starch accumulation is altered in *pht2;1* and *pht4;4* leaves. Leaves were harvested at end of the photoperiod, n=5.

Expression of *PHT2;1* and *PHT4;4* is elevated in the *tpt* mutant background

The *tpt* mutant did not show any obvious growth defect under standard growth conditions, which may be due to functional redundancy or compensation that involves PHT2;1 and/or PHT4;4. To determine whether compensation at the transcript level exists in the *tpt* background, I used quantitative RT-PCR to assess transcript levels of *PHT2;1* and each of the PHT4 genes that encode plastid-localized proteins. *PHT4;4* transcript levels were increased 3-fold while *PHT2;1* increased 5-fold in the *tpt* background relative to wild type (Fig. 24). This suggests that in the absence of *tpt*, PHT2;1 and PHT4;4 fulfill the Pi demands of the chloroplast.

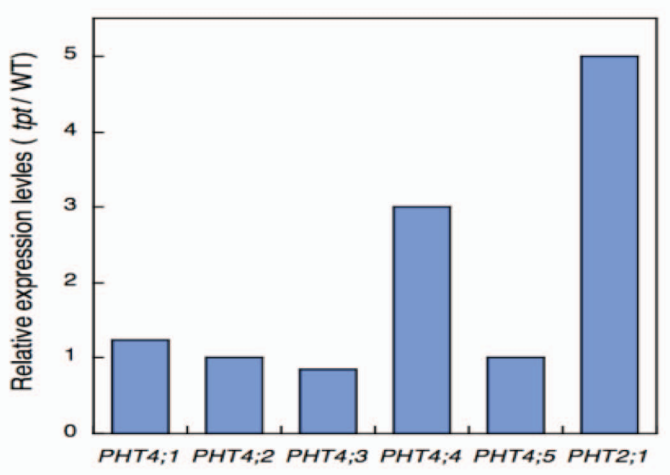

Figure 24. PHT4;4 and PHT2;1 expression is elevated in the *tpt* mutant background. Transcript levels were determined by quantitative RT-PCR and *EIF-4A* was used for normalization.

Isolation of plants with multiple chloroplast Pi transport mutations

I initially hypothesized that PHT4;4, PHT2;1 and TPT are the sole routes for Pi transport into the chloroplast and that plants that lack two or all three of these proteins may show additive effects or synthetic lethality. I isolated plants with all possible combinations of *pht2;1*, *pht4;4*and *tpt* mutations. Although the double and triple mutants have not been investigated in detail, some interesting observations have been made. For example, the triple mutant is viable, which indicates that additional mechanisms for Pi import exist. However, these mechanisms may have minor roles because growth of the triple mutant is reduced (Fig. 25) and flowering is delayed. Also, the triple mutant is pale and has significantly less chlorophyll a and b (Fig. 26), which is not observed in any of the other mutants.

Rosette Area in cm^2	
Wild type	24.83 ± 1.70
pht2;1 pht4;4 tpt	10.05 ± 0.46

Figure 25. Size phenotype of *pht2;1 pht4;4 tpt* triple mutant. Plants were grown for 8 weeks.

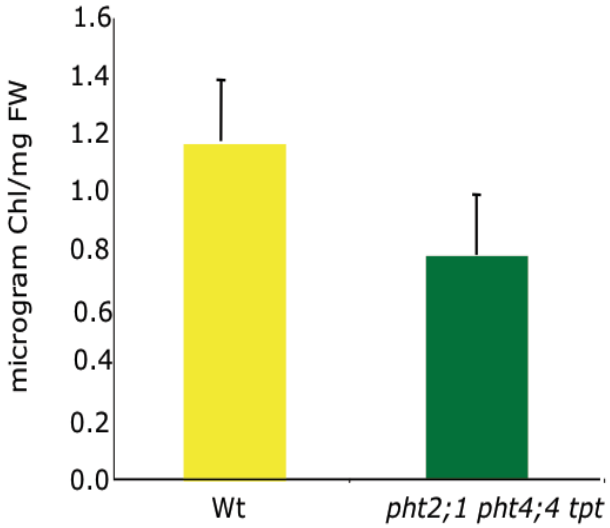

Figure 26. A *pht2;1 pht4;4 tpt* mutant has reduced levels of Chl a and Chl b. Plants were grown 6 weeks with 8 hr photoperiod and 60 µmol m^{-2} s^{-1} light intensity. n= 7, $p < 0.05$.

Discussion

Pi homeostasis in plants is a complex process because there are several mechanisms involved in maintaining the internal Pi balance of the cell, including biochemical changes and molecular changes like changes in chromatin structure (Smith et al., 2010) and up-regulation of Pi transporter genes (Flügge and Heldt, 1993; Raghothama, 1999). It is not possible to examine all factors contributing to Pi homeostasis at once, so my work focused on the role of Pi transporters that play a major role in balancing the level of Pi in the chloroplast. Most of chloroplast Pi transporters are antiporters (details in Chapter I), but there are several others like members of the PHT4

and PHT2 families whose functions are still not known completely. In this work, attempts were made to understand the role of PHT4;4 and PHT2;1 transporters and their contribution to Pi homeostasis.

Preliminary analyses showed that *pht2;1*, *pht4;4* and *pht2;1 pht4;4 tpt* (triple) mutants have different growth phenotypes under defined conditions of photoperiod and light intensity. To interpret these phenotypes in terms of the physiology and mechanism of the affected transporters, the growth and development of plants that carry all combinations of *tpt*, *pht2;1* and *pht4;4* mutations can be evaluated under conditions of both short (8 hrs.) and long (14 hrs.) photoperiod and with low, standard and high light intensities. The phenotypic comparisons will allow us to determine if any of the double mutant combinations are additive.

Starch measurements for *pht2;1* and *pht4;4* at the end of photoperiod (Fig. 22) were consistent with the idea that mutants with defects in Pi import will result in increased starch levels at the expense of soluble sugars, and that mutants with defects in Pi export will show the opposite starch accumulation pattern. Starch quantification can be done for all of the mutants at the beginning, midpoint and end of the photoperiod, and starch and soluble sugar contents can be quantified using standard assays (Corbesier et al., 1998; Smith and Zeeman, 2006). Because starch synthesis recycles Pi inside the stroma, and thus may mask some deficiencies in Pi import, introducing the starch deficient mutant *aps-1 or adg-1* into the *pht2;1* and *pht4;4* backgrounds might circumvent this issue. It is expected that the inability to recycle Pi will make *pht2;1* and/or *pht4;4* defects in Pi import more pronounced. This idea is supported by the

observation that growth of a *tpt adg-1* (*adg-1* is unable to synthesize starch) double mutant is severely impaired (Schneider et al., 2002). If the double mutants of *pht4;4 aps-1* or *pht2;1 aps* also show a severe growth phenotype, it would suggest that the affected unidirectional Pi transporter contributes to chloroplast Pi import.

It is possible that the starch accumulation patterns of *pht2;1* and *pht4;4* plants reflect a difference in regulation rather than transport direction. *PHT2;1* is rapidly induced by light and its expression peaks early in the photoperiod, whereas *PHT4;4* expression rises after 3 hrs of light and peaks in the latter half of the photoperiod (Guo et al., 2008a). To test this possibility, a promoter swapping approach can be done to test whether *PHT4;4* driven by a *PHT2;1* promoter complements the *pht2;1* phenotype, and whether *PHT2;1* driven by a *PHT4;4* promoter complements the *pht4;4* phenotype. Complementation would suggest that the respective transport activities are redundant. Failure to compliment would support the idea that these proteins have different, import vs. export, activities.

Photosynthetic studies with isolated chloroplasts demonstrated that Pi is required for photosynthesis due, at least in part, to its requirement for photophosphorylation (Walker and Sivak, 1986). Photosynthetic analyses of the mutants can be done to monitor CO_2 assimilation for each genotype. Results from these experiments will reveal potential photosynthetic limitations and allow distinction between the limitations associated with ribulose bisphosphate (RuBP) regeneration and triose phosphate utilization. The hypothesis is that RuBP regeneration will be a limiting factor for CO2 assimilation if the mutations reduce the Pi supply to chloroplast, whereas if the

mutations prevent export of excess stromal Pi, triose–P utilization may be limiting (Sharkey et al., 2007). Chlorophyll fluorescence may also be analyzed for some of the genotypes to quantify nonphotochemical quench, which may be sensitive to stromal Pi levels (Takizawa et al., 2008).

Increased expression of *PHT4;4* and *PHT2;1* in the *tpt* mutant background (Fig. 23) suggests compensation. It is also possible that compensatory transport activities are responsible for the viability of the *pht2;1 pht4;4 tpt* triple mutant. In each case, compensation would strongly influence our interpretation of mutant phenotypes and analysis of transport activities in isolated chloroplast vesicles. A systematic analysis of chloroplast Pi transporter gene expression in each of the genotypes can be done, including measurement of transcript levels for *PHT2;1*, *PHT4;4*, *TPT* and each of other the members of pPT family, xylulose-5-phosphate/Pi translocator (*XPT*), glucose-6-phosphate/Pi translocator (*GPT*), phosphoenolpyruvate/Pi traslocator (*PPT*). Although these additional pPT members normally mediate Pi export from chloroplasts and non-green plastids (Knappe et al., 2003; Weber et al., 2004), each is capable of passive, bi-directional Pi transport *in vitro* (Nozawa et al., 2007). Thus it is possible that these translocators contribute to Pi import when mutations render such transport favorable.

I proposed that PHT4;4 mediates Pi export from the chloroplast based on the reduced starch accumulation phenotype of the *pht4;4* mutant. However, if transport occurs via a passive mechanism, then import could also occur if the electrochemical gradient for Pi is favorable. Such a situation may occur in some mutant backgrounds. To address whether PHT4;4, as well as PHT2;1, mediates active or passive Pi transport, *in*

vitro transport assays can be conducted using vesicles made from the chloroplast inner envelope. This approach has been used successfully for a variety of other ions (Berkowitz and Peters, 1993; Shingles and McCarty, 1995; Shingles et al., 1996; Shingles et al., 2001; Shingles et al., 2002). Antibodies for proteins in the inner (Tic110) and outer (Toc75) membrane can be used to evaluate yield and orientation of vesicles prepared from Arabidopsis chloroplasts following established procedures (Keegstra and Yousif, 1986; Shingles et al., 2002). Transport assays can be done with the vesicles prepared from the *tpt pht2;1* and *tpt pht4;4* double mutants to analyze the activity of the PHT4;4 and PHT2;1, respectively. Vesicles prepared from the *tpt pht2;1 pht4;4* triple mutant will be used to establish the background transport activity. The concentration of Pi inside and outside the vesicles can be varied as needed to determine whether transport against a concentration gradient (active) occurs. Transport will be monitored using ^{32}Pi, and radioactivity will be measured using a liquid scintillation counter.

If problems arise with the vesicle system, reconstituted proteoliposomes may be used as an alternative approach. Reconstituted proteoliposomes have been used previously to monitor transport activities of pPT proteins (Renne et al., 2003; Bouvier et al., 2006), but orientation of the protein within the liposome would be random. This may complicate analysis of unidirectional transport.

Another fascinating fact that has not been the focus of the current work was to demonstrate in detail the cause of the bigger size phenotype shown by *pht4;4* mutants. Although this work reveled that the large size of *pht4;4* mutants is due to an increased number of cells, it is still unknown which metabolic signaling events are triggered to

contribute to the regulation of cell proliferation and final leaf size. A mutant of another member of PHT4 family called PHT4;2 also shows a large-size phenotype when grown under short photoperiods. Unlike PHT4;4, PHT4;2 is present in root plastids. Interestingly, the effects of the mutations on leaf size in a *pht4;2 pht4;4* double mutant are additive, which is indicative of independent mechanisms for regulating cell number. It will be interesting to determine the mechanisms through which plastidic Pi homeostasis influences leaf size.

Materials and Methods

Plant growth conditions

Plants were grown in chambers at 21°C with 70% relative humidity and an 8 h photoperiod (150 μmol m^{-2} s^{-1}) in potting medium (SunGro Redi-earth, Bellevue, WA). Insertion sites and zygosity were confirmed by PCR using combinations of *PHT4;4*-specific primers and primers that anneal to the T-DNA right and left borders. The sequence of amplicons that spanned insertion junctions was confirmed.

Cell size analysis

The area of rosettes and individual rosette leaves was determined from digital images that included reference objects using the histogram function of Adobe Photoshop. To determine epidermal cell area, nail polish impressions of the abaxial epidermis were prepared from the ninth rosette leaf of at least three wild-type and *pht4;4-1* plants. Images were captured for three different locations in each leaf between

25% and 75% of the distance between the tip and the base of the blade, halfway between the mid-rib and leaf margin. Cells in each field of view were counted, and cell areas (mean ± SE) were determined from a total of at least 500 cells.

Extraction and measurement of starch

Leaf and root samples were harvested at the end of the photoperiod then immediately frozen in liquid nitrogen. Starch was extracted with 80% (v/v) ethanol, 5% (v/v) formic acid at 80^{o}C for 20 min then the extraction was repeated with 80% ethanol. The supernatants were pooled, lyophilized, suspended in 10 mM Na-acetate (pH 5.5) then assayed for Suc. Pellets were dried and starch was gelatinized and hydrolyzed as described (Smith and Zeeman, 2006). Starch concentrations were quantified using coupled assays in which the formation of NADH was monitored by absorbance at 340 nm using a Synergy HT microplate reader. All assays were performed in duplicate and values were determined from standard curves. At least four independent samples were collected for each time point and results are reported as mean ± SE.

RT-PCR analysis

Total RNA was isolated from leaves using TRI reagent (Sigma Aldrich, St. Louis, MO), and traces of DNA were eliminated with the TURBO DNA-free kit (Ambion, Austin, TX). First-strand cDNA was synthesized using SuperScript first-strand cDNA synthesis kit (Invitrogen, Carlsbad, CA). RT-PCR was conducted using primers that align downstream of the Ds transposon insertion. RT-PCR with primers specific to

EIF-4A2 was used an RNA input control.

Measurement of chlorophyll content

Fresh plant tissue (0.1–0.2 g) was crushed with a micropestle in liquid nitrogen then 1 ml of 80% acetone was added to tube, mixed briefly and the supernatant was transferred to a new tube. An additional 1 ml of acetone to was added to the ground tissue and mixed briefly and the supernatants were combined. Samples were centrifuged for 10 min at 4°C. Supernatant was transferred to a fresh tube and kept on ice. The same process was repeated until the pellet was completely white. Chlorophyll a, b, and a/b ratios were quantified from the absorbance values at 663.6 and 646.6 nm as described (Arnon, 1949), following the equations listed below.

Chl A= $12.21(A_{663.6})- 2.81(A_{646.6})$

Chl B= $20.13(A_{646.6})- 5.03(A_{663.6})$

Chl_{total}= Chl A + Chl B

$$\frac{(\text{Chl total})\ (\text{Total volume in ml})}{(\text{Fresh weight in grams})\ (1000)} = \frac{\mu\text{g Chl}}{\text{mg}}$$

CHAPTER IV

CONCLUSION AND FUTURE DIRECTIONS

With the development of the new technologies, the use of biosensors has revolutionized biological research (Frommer et al., 2009). Wide ranges of fluorescent protein variants have enabled imaging technologies like FRAP (Fluorescence Recovery After Photobleaching), FLIM (Fluorescence lifetime imaging) and confocal microscopy (Soumpasis, 1983; Kwak et al., 2001). Genetically encoded fluorescent biosensors have been successfully used to report analytes, ions, and metabolites in cells in real time (Jaeger et al., 1999; Leveau and Lindow, 2002; Fehr et al., 2004; Deuschle et al., 2005; Chaudhuri et al., 2011). These sensors have also been used for pH measurements in the cells, for example pHusion (Gjetting et al., 2012) and pHluorin (Certal et al., 2008) in plant cytosol. The list of all currently available biosensors and their functions can be found at http://biosensor.dpb.carnegiescience.edu/ (Okumoto et al., 2012).

I constructed a collection of Pi sensors, cpFLIPPi sensors, for real time quantitative detection of Pi in live cells. As discussed in Chapter III, an important goal is to assess steady state Pi levels for chloroplasts of Arabidopsis wild-type, *pht2;1* and *pht4;4* plants. This will give an unambiguous answer to the proposed model for PHT2;1 and PHT4;4 transport function. The cpFLIPPi sensors, specifically cpFLIPPi-6.4m can be used to quantify a ratiometric Pi-dependent FRET response when introduced into mutant and wild-type chloroplasts. I predict that *pht4;4* mutants will show a low FRET ratio (cpVenus/CFP) indicating high Pi levels in the stroma, whereas *pht2;1* mutants will

show a higher FRET ratio consistent with low stromal Pi. Similarly, Pi levels can be measured in other mutant combinations (double and triple mutants) to achieve a better understanding of the role of individual plastidic transporters in Pi homeostasis.

These sensors can also be used to evaluate the cell-to-cell variance in cytosolic Pi. Pi concentration variations in different regions of the plant (epidermal, cortical) or different organs like root, shoot and leaves can be analyzed. Similarly, the variations in Pi concentrations in the plastids, within and between individual cells can also be determined. cpFLIPPi sensors can be used to track Pi changes during diurnal cycle or changes pertaining to different abiotic environmental conditions (example, high or low sucrose/mannose availability etc.).

FRET-based sensors have proved to be a promising tool for metabolite detection, but application of these sensors in plants has been limited compared to mammalian cells (Gjetting et al., 2013). Gene silencing is a major limitation for the use of fluorescent sensors in plants, but use of silencing mutations can over-come this problem (Chapter II). Time-consuming empirical studies are required to optimize ligand affinity, but I have shown that SCA greatly enhances the efficiency of a ligand affinity mutant screen, and this approach is likely to be broadly applicable.

Development of New Sensors

FRET-based sensors are the most commonly used type of sensors (Deuschle et al., 2005; Gjetting et al., 2013). The choice of FRET pairs has expanded recently and many new flurophore combinations are available, like GFP/mCherry (Tramier et al.,

2006), sapphire/RFP (Shcherbo et al., 2009), mOrange/mCherry (Piljic and Schultz, 2008), TagRFP/mPlum (Grant et al., 2008) and aAmetrine/TdTomato (Ai et al., 2008). The optimization of alternative FRET pairs for use in plants will enable simultaneous monitoring of more than one analyte or a single analyte in more than one cell location.

Another type of sensor called single fluorophore sensors, has also been used for metabolite detection and reporting. Single fluorophore sensors consist of a ligand-binding domain fused to a single flurophore protein. These sensors have an advantage over FRET-based sensors due to simple detection and ease of use because data acquisition can be done at a single wavelength, thus avoiding bleedthrough issues. Many single fluorophore sensors have been reported to have higher dynamic ranges than FRET-based sensors (Akerboom et al., 2009). The major limitation for single fluorophore sensors is that development typically involves greater manipulation because either the ligand binding domain or the fluorescent protein has to be split to allow insertion of other (Deuschle et al., 2005; Okumoto et al., 2005; Gu et al., 2006). Insertion of a fluorescent protein into a recognition domain might inhibit appropriate protein folding. Because the readout from this type of sensor is at single emission wavelength, artifacts can be generated due to changes in spectral properties. Rearranging the sequential order of fluorescent proteins and sensory domain can circumvent this problem.

As most of the Pi is reported to be stored in the vacuole (Abel et al., 2002)**,** development of Pi sensors for monitoring Pi concentrations in vacuoles can serve as a useful tool. The pH of the large central vacuole in plant cells is ~5.5 (Bassil et al., 2011).

In my preliminary experiments I found that only one of the Pi sensors currently in hand (cpFLIPPi-11m) exhibits a Pi-dependent FRET signal at this pH, but the magnitude of the response is very small. More suitable sensors for monitoring vacuolar Pi contents may be identified from a screen of our existing population of mutated sensor plasmids. In the process of screening I also found that there are several mutants that do not show a FRET response with varied Pi concentration, but do have good absolute fluorescence intensity values for CFP and cpVenus. Although these sensors are not responsive to Pi, they may be a well suited for measuring viscosity of the cells. In all our assays, pseudocytosol includes 40% sucrose to simulate cell viscosity. Previous experiments in which sucrose concentration was varied suggested that increasing viscosity suppresses FRET of FLIPPi-200μ, but the Pi-dependent response is maintained. To ensure that any changes we observe are due to viscosity in general rather than a specific response to sucrose we can test the effect of the polymer Ficoll 400 (Pocker and Janjic, 1987).

LITERATURE CITED

Abel S, Ticconi CA, Delatorre CA (2002) Phosphate sensing in higher plants. Physiologia Plantarum **115:** 1-8

Adams JP, Adeli A, Hsu CY, Harkess RL, Page GP, Depamphilis CW, Schultz EB, Yuceer C (2012) Plant-based FRET biosensor discriminates environmental zinc levels. Plant Biotechnology Journal **10:** 207-216

Ai H-w, Hazelwood KL, Davidson MW, Campbell RE (2008) Fluorescent protein FRET pairs for ratiometric imaging of dual biosensors. Nature Methods **5:** 401-403

Akerboom J, Rivera JD, Guilbe MM, Malave EC, Hernandez HH, Tian L, Hires SA, Marvin JS, Looger LL, Schreiter ER (2009) Crystal structures of the GCaMP calcium sensor reveal the mechanism of fluorescence signal change and aid rational design. Journal of Biological Chemistry **284:** 6455-6464

Altschul SF, Madden TL, Schäffer AA, Zhang J, Zhang Z, Miller W, Lipman DJ (1997) Gapped BLAST and PSI-BLAST: a new generation of protein database search programs. Nucleic Acids Research **25:** 3389-3402

Arnon DI (1949) Copper enzymes in isolated chloroplasts polyphenoloxidase in *Beta Vulgaris*. Plant Physiology **24:** 1-15

Ballicora MA, Iglesias AA, Preiss J (2004) ADP-glucose pyrophosphorylase: a regulatory enzyme for plant starch synthesis. Photosynthesis Research **79:** 1-24

Barnes SA, Knight JS, Gray JC (1994) Alteration of the amount of the chloroplast phosphate translocator in transgenic tobacco affects the distribution of assimilate between starch and sugar. Plant Physiology **106:** 1123-1129

Bassil E, Tajima H, Liang Y-C, Ohto M-a, Ushijima K, Nakano R, Esumi T, Coku A, Belmonte M, Blumwald E (2011) The Arabidopsis Na+/H+ antiporters

NHX1 and NHX2 control vacuolar pH and K+ homeostasis to regulate growth, flower development, and reproduction. Plant Cell **23:** 3482-3497

Berkowitz GA, Peters JS (1993) Chloroplast inner-envelope ATPase acts as a primary H^+ pump. Plant Physiology **102:** 261-267

Bieleski RL (1973) Phosphate pools, phosphate transport and phosphate availability. Annual Review of Plant Physiology **24:** 225-252

Bouvier F, Linka N, Isner JC, Mutterer J, Weber AP, Camara B (2006) Arabidopsis SAMT1 defines a plastid transporter regulating plastid biogenesis and plant development. Plant Cell **18:** 3088-3105

Cardenas L, Lovy-Wheeler A, Kunkel JG, Hepler PK (2008) Pollen tube growth oscillations and intracellular calcium levels are reversibly modulated by actin polymerization. Plant Physiology **146:** 1611-1621

Certal AC, Almeida RB, Carvalho LM, Wong E, Moreno N, Michard E, Carneiro J, Rodriguéz-Léon J, Wu H-M, Cheung AY, Feijó JA (2008) Exclusion of a proton ATPase from the apical membrane is associated with cell polarity and tip growth in Nicotiana tabacum pollen tubes. Plant Cell **20:** 614-634

Chaudhuri B, Hormann F, Frommer WB (2011) Dynamic imaging of glucose flux impedance using FRET sensors in wild-type Arabidopsis plants. Journal of Experimental Botany **62:** 2411-2417

Chaudhuri B, Hörmann F, Lalonde S, Brady SM, Orlando DA, Benfey P, Frommer WB (2008) Protonophore- and pH-insensitive glucose and sucrose accumulation detected by FRET nanosensors in Arabidopsis root tips. Plant Journal **56:** 948-962

Chiou TJ, Lin SI (2011) Signaling network in sensing phosphate availability in plants. Annual Review of Plant Biology **62:** 185-206

Clough SJ, Bent AF (1998) Floral dip: a simplified method forAgrobacterium-mediated transformation of *Arabidopsis thaliana*. Plant Journal **16:** 735-743

Copeland L, Zammit A (1994) Kinetic properties of NAD-Dependent glyceraldehyde-3-phosphate dehydrogenase from the host fraction of Soybean root nodules. Archives of Biochemistry and Biophysics **312:** 107-113

Corbesier L, Lejeune P, Bernier G (1998) The role of carbohydrates in the induction of flowering in *Arabidopsis thaliana*: comparison between wild type and a starchless mutant. Planta **206:** 131-137

Cubero B, Nakagawa Y, Jiang XY, Miura KJ, Li F, Raghothama KG, Bressan RA, Hasegawa PM, Pardo JM (2009) The phosphate transporter PHT4;6 is a determinant of salt tolerance that is localized to the Golgi apparatus of Arabidopsis. Molecular Plant **2:** 535-552

Daram P, Brunner S, Rausch C, Steiner C, Amrhein N, Bucher M (1999) *Pht2;1* encodes a low-affinity phosphate transporter from Arabidopsis. Plant Cell **11:** 2153-2166

Demmig B, Gimmler H (1983) Properties of the isolated intact chloroplast at cytoplasmic K concentrations: I. light-induced cation uptake into intact chloroplasts is driven by an electrical potential difference. Plant Physiology **73:** 169-174

Desmoulin F, Cozzone PJ, Canioni P (1987) Phosphorus-31 nuclear-magnetic-resonance study of phosphorylated metabolites compartmentation, intracellular pH and phosphorylation state during normoxia, hypoxia and ethanol perfusion, in the perfused rat liver. European Journal of Biochemistry **162:** 151-159

Deuschle K, Chaudhuri B, Okumoto S, Lager I, Lalonde S, Frommer WB (2006) Rapid metabolism of glucose detected with FRET glucose nanosensors in epidermal cells and intact roots of Arabidopsis RNA-silencing mutants. Plant Cell **18:** 2314-2325

Deuschle K, Okumoto S, Fehr M, Looger LL, Kozhukh L, Frommer WB (2005) Construction and optimization of a family of genetically encoded metabolite sensors by semirational protein engineering. Protein Science **14:** 2304-2314

Edgar RC (2004) MUSCLE: multiple sequence alignment with high accuracy and high throughput. Nucleic Acids Research **32:** 1792-1797

Fehr M, Ehrhardt DW, Lalonde S, Frommer WB (2004) Minimally invasive dynamic imaging of ions and metabolites in living cells. Current Opinion in Plant Biology **7:** 345-351

Feijó JA, Sainhas J, Hackett GR, Kunkel JG, Hepler PK (1999) Growing pollen tubes possess a constitutive alkaline band in the clear zone and a growth-dependent acidic tip. Journal of Cell Biology **144:** 483-496

Ferro M, Salvi D, Riviere-Rolland H, Vermat T, Seigneurin-Berny D, Grunwald D, Garin J, Joyard J, Rolland N (2002) Integral membrane proteins of the chloroplast envelope: identification and subcellular localization of new transporters. Proceedings of the National Academy of Sciences **99:** 11487-11492

Fischer K, Kammerer B, Gutensohn M, Arbinger B, Weber A, Häusler RE, Flügge UI (1997) A new class of plastidic phosphate translocators: a putative link between primary and secondary metabolism by the phosphoenolpyruvate/phosphate antiporter. Plant Cell **9:** 453-462

Flügge UI (1998) Metabolite transporters in plastids. Current Opinion in Plant Biology **1:** 201-206.

Flügge UI (1999) Phosphate translocators in plastids. Annual Review of Plant Physiology and Plant Molecular Biology. **50:** 27-45

Flügge UI (2003) Functional genomics of phosphate antiport systems in plastids. Physiologia Plantarum **118:** 475-482

Flügge UI, Fischer K, Gross A, Sebald W, Lottspeich F, Eckerskorn C (1989) The triose phosphate-3-phosphoglycerate-phosphate translocator from spinach chloroplasts: nucleotide sequence of a full-length cDNA clone and import of the in vitro synthesized precursor protein into chloroplasts. EMBO Journal **8:** 39-46

Flügge UI, Heldt HW (1984) The phosphate-triose phosphate-phosphoglycerate translocator of the chloroplast. Trends in Biochemical Sciences **9:** 530-533

Flügge UI, Heldt HW (1993) Metabolite translocators of the chloroplast envelope. Annual Review of Plant Physiology and Plant Molecular Biology **42:** 129-144

Förster T (1948) Zwischenmolekulare Energiewanderung und Fluoreszenz. Annalen der Physik **437:** 55-75

Frommer WB, Davidson MW, Campbell RE (2009) Genetically encoded biosensors based on engineered fluorescent proteins. Chemical Society Reviews **38:** 2833-2841

Geigenberger P, Tiessen A, Meurer J (2011) Use of non-aqueous fractionation and metabolomics to study chloroplast function in Arabidopsis. Methods in Molecular Bioliogy **775:** 135-160

Geldner N, Dénervaud-Tendon V, Hyman DL, Mayer U, Stierhof Y-D, Chory J (2009) Rapid, combinatorial analysis of membrane compartments in intact plants with a multicolor marker set. Plant Journal **59:** 169-178

Gerhardt R, Heldt HW (1984) Measurement of subcellular metabolite levels in leaves by fractionation of freeze-stopped material in nonaqueous media. Plant Physiology **75:** 542-547

Gerhardt R, Stitt M, Heldt HW (1987) Subcellular metabolite levels in spinach leaves. Plant Physiology **83:** 399-407

Gibon Y, Blasing OE, Palacios-Rojas N, Pankovic D, Hendriks JH, Fisahn J, Hohne M, Gunther M, Stitt M (2004) Adjustment of diurnal starch turnover to short days: depletion of sugar during the night leads to a temporary inhibition of carbohydrate utilization, accumulation of sugars and post-translational activation of ADP-glucose pyrophosphorylase in the following light period. Plant Journal **39:** 847-862

Gjetting KS, Ytting CK, Schulz A, Fuglsang AT (2012) Live imaging of intra- and extracellular pH in plants using pHusion, a novel genetically encoded biosensor. Journal of Experimental Botany **63:** 3207-3218

Gjetting SK, Schulz A, Fuglsang AT (2013) Perspectives for using genetically encoded fluorescent biosensors in plants. Frontiers in Plant Science **4:** 234-237

Gout E, Bligny R, Douce R, Boisson A-M, Rivasseau C (2011) Early response of plant cell to carbon deprivation: in vivo31P-NMR spectroscopy shows a quasi-instantaneous disruption on cytosolic sugars, phosphorylated intermediates of energy metabolism, phosphate partitioning, and intracellular pHs. New Phytologist **189:** 135-147

Grant DM, Zhang W, McGhee EJ, Bunney TD, Talbot CB, Kumar S, Munro I, Dunsby C, Neil MAA, Katan M, French PMW (2008) Multiplexed FRET to image multiple signaling events in live cells. Biophysical Journal **95:** L69-L71

Grefen C, Donald N, Hashimoto K, Kudla J, Schumacher K, Blatt MR (2010) A ubiquitin-10 promoter-based vector set for fluorescent protein tagging facilitates temporal stability and native protein distribution in transient and stable expression studies. Plant Journal **64:** 355-365

Gu H, Lalonde S, Okumoto S, Looger LL, Scharff-Poulsen AM, Grossman AR, Kossmann J, Jakobsen I, Frommer WB (2006) A novel analytical method for in vivo phosphate tracking. FEBS Letters **580:** 5885-5893

Guo B, Irigoyen S, Fowler TB, Versaw WK (2008b) Differential expression and phylogenetic analysis suggest specialization of plastid-localized members of the PHT4 phosphate transporter family for photosynthetic and heterotrophic tissues. Plant Signalling & Behaviour **3:** 784-790

Guo B, Jin Y, Wussler C, Blacaflor EB, Motes CM, Versaw WK (2008a) Functional analysis of the Arabidopsis PHT4 family of intracellular phosphate transporters. New Phytologist **177:** 889-898

Heldt HW, Sauer F (1971) The inner membrane of the chloroplast envelope as the site of specific metabolite transport. Biochimica et Biophysica Acta **234:** 83-91

Irigoyen S, Karlsson PM, Kuruvilla J, Spetea C, Versaw WK (2011) The sink-specific plastidic phosphate transporter PHT4;2 influences starch accumulation and leaf size in Arabidopsis. Plant Physiology **157:** 1765-1777

Jaeger CH, Lindow SE, Miller W, Clark E, Firestone MK (1999) Mapping of sugar and amino acid availability in soil around roots with bacterial sensors of sucrose and tryptophan. Applied and Environmental Microbiology **65:** 2685-2690

Jain A, Nagarajan V, Raghothama K (2012) Transcriptional regulation of phosphate acquisition by higher plants. Cellular and Molecular Life Sciences **69:** 3207-3224

Jose M, Nair DK, Reissner C, Hartig R, Zuschratter W (2007) Photophysics of Clomeleon by FLIM: discriminating excited state reactions along neuronal development. Biophysical Journal **92:** 2237-2254

Kammerer B, Fischer K, Hilpert B, Schubert S, Gutensohn M, Weber A, Flügge UI (1998) Molecular characterization of a carbon transporter in plastids from heterotrophic tissues: the glucose 6-phosphate/phosphate antiporter. Plant Cell **10:** 105-117

Kaper T, Lager I, Looger L, Chermak D, Frommer W (2008) Fluorescence resonance energy transfer sensors for quantitative monitoring of pentose and disaccharide accumulation in bacteria. Biotechnology for Biofuels **1:** 1-11

Karley AJ, Leigh RA, Sanders D (2000) Differential ion accumulation and ion fluxes in the mesophyll and epidermis of Barley. Plant Physiology **122:** 835-844

Keegstra K, Yousif AE (1986) Isolation and characterization of chloroplast envelope membranes. Methods in Enzymology **118:** 316-325

Knappe S, Flügge UI, Fischer K (2003) Analysis of the plastidic *phosphate translocator* gene family in Arabidopsis and identification of new phosphate translocator-homologous transporters, classified by their putative substrate-binding site. Plant Physiology **131:** 1178-1190

Krebs M, Held K, Binder A, Hashimoto K, Den Herder G, Parniske M, Kudla J, Schumacher K (2012) FRET-based genetically encoded sensors allow high-resolution live cell imaging of Ca(2)(+) dynamics. Plant Journal **69:** 181-192

Kumakura N, Takeda A, Fujioka Y, Motose H, Takano R, Watanabe Y (2009) SGS3 and RDR6 interact and colocalize in cytoplasmic SGS3/RDR6-bodies. FEBS Letters **583:** 1261-1266

Kwak E-S, Kang TJ, Vanden Bout DA (2001) Fluorescence lifetime imaging with near-field scanning optical microscopy. Analytical Chemistry **73:** 3257-3262

Lager I, Looger LL, Hilpert M, Lalonde S, Frommer WB (2006) Conversion of a putative Agrobacterium sugar-binding protein into a FRET sensor with high selectivity for sucrose. Journal of Biological Chemistry **281:** 30875-30883

Lalonde S, Ehrhardt DW, Frommer WB (2005) Shining light on signaling and metabolic networks by genetically encoded biosensors. Current Opinion in Plant Biology **8:** 574-581

Lee DW, Lee S, Lee GJ, Lee KH, Kim S, Cheong GW, Hwang I (2006) Functional characterization of sequence motifs in the transit peptide of Arabidopsis small subunit of rubisco. Plant Physiology **140:** 466-483

Lee RB, Ratcliffe RG (1993) Subcellular distribution of inorganic phosphate, and levels of nucleoside triphosphate, in mature maize roots at low external phosphate concentrations: Measurements with ^{31}P-NMR. Journal of Experimental Botany **44:** 587-598

Lejay L, Wirth J, Pervent M, Cross JM, Tillard P, Gojon A (2008) Oxidative pentose phosphate pathway-dependent sugar sensing as a mechanism for regulation of root ion transporters by photosynthesis. Plant Physiology **146:** 2036-2053

Leveau JHJ, Lindow SE (2002) Bioreporters in microbial ecology. Current Opinion in Microbiology **5:** 259-265

Lockless SW (1999) Evolutionarily conserved pathways of energetic connectivity in protein families. Science **286:** 295-299

Looger LL, Lalonde S, Frommer WB (2005) Genetically encoded FRET sensors for visualizing metabolites with subcellular resolution in living cells. Plant Physiology **138:** 555-557

Lopez-Juez E, Pyke KA (2005) Plastids unleashed: their development and their integration in plant development. International Journal of Developmental Bioliogy **49:** 557-577

Loughman BC, Ratcliffe RG, Southon TE (1989) Observations on the cytoplasmic and vacuolar orthophosphate pools in leaf tissues using in vivo 31P-NMR spectroscopy. FEBS Letters **242:** 279-284

Lynch J (1995) Root architecture and plant productivity. Plant Physiology **109:** 7-13

Marschner H, Kirkby EA, Cakmak I (1996) Effect of mineral nutritional status on shoot-root partitioning of photoassimilates and cycling of mineral nutrients. Journal of Experimental Botany **47:** 1255-1263

Martel S, Clement JL, Muller A, Culcasi M, Pietri S (2002) Synthesis and 31P NMR characterization of new low toxic highly sensitive pH probes designed for in vivo acidic pH studies. Bioorganic and Medicinal Chemistry **10:** 1451-1458

Messerli MA, Robinson KR (1998) Cytoplasmic acidification and current influx follow growth pulses of *Lilium longiflorum* pollen tubes. Plant Journal **16:** 87-91

Mimura T (1995) Homeostasis and transport of inorganic phosphate in plants. Plant and Cell Physiology **36:** 1-7

Mimura T (1999) Regulation of phosphate transport and homeostasis in plant cells. International Review of Cytology **191:** 149-200

Miyawaki A, Griesbeck O, Heim R, Tsien RY (1999) Dynamic and quantitative Ca2+ measurements using improved cameleons. Proceedings of the National Academy of Sciences **96:** 2135-2140

Muchhal US, Pardo JM, Raghathama KG (1996) Phosphate transporters from the higher plant *Arabidopsis thaliana*. Proceedings of the National Academy of Sciences **93:** 101519-110523

Mudge SR, Rae AL, Diatloff E, F.W. S (2002) Expression analysis suggests novel roles for members of the Pht1 family of phosphate transporters in Arabidopsis. Plant Journal. **31:** 341-353

Nagai T, Ibata K, Park ES, Kubota M, Mikoshiba K, Miyawaki A (2002) A variant of yellow fluorescent protein with fast and efficient maturation for cell-biological applications. Nature Biotechnology **20:** 87-90

Nagai T, Yamada S, Tominaga T, Ichikawa M, Miyawaki A (2004) Expanded dynamic range of fluorescent indicators for $Ca(^{2+})$ by circularly permuted yellow fluorescent proteins. Proceedings of the National Academy of Sciences **101:** 10554-10559

Neuhaus HE, Emes MJ (2000) Nonphotosynthetic metabolism in plastids. Annual Review of Plant Physiology and Plant Molecular Biology **51:** 111-140

Neuhaus HE, Maass U (1996) Unidirectional transport of orthophosphate across the envelope of isolated cauliflower-bud amyloplasts. Planta **198:** 542-548

Neuhaus HE, Wagner R (2000) Solute pores, ion channels, and metabolite transporters in the outer and inner envelope membranes of higher plant plastids. Biochimica et Biophysica Acta **1465:** 307-323

Nielsen TH, Krapp A, Röper-Schwarz U, Stitt M (1998) The sugar-mediated regulation of genes encoding the small subunit of Rubisco and the regulatory subunit of ADP glucose pyrophosphorylase is modified by phosphate and nitrogen. Plant, Cell & Environment **21:** 443-454

Norris S, Meyer S, Callis J (1993) The intron of *Arabidopsis thaliana* polyubiquitin genes is conserved in location and is a quantitative determinant of chimeric gene expression. Plant Molecular Biology **21:** 895-906

Nozawa A, Nanamiya H, Miyata T, Linka N, Endo Y, Weber AP, Tozawa Y (2007) A cell-free translation and proteoliposome reconstitution system for functional analysis of plant solute transporters. Plant and Cell Physiology **48:** 1815-1820

Okumoto S, Jones A, Frommer WB (2012) Quantitative imaging with fluorescent biosensors. Annual Review of Plant Biology **63:** 663-706

Okumoto S, Looger LL, Micheva KD, Reimer RJ, Smith SJ, Frommer WB (2005) Detection of glutamate release from neurons by genetically encoded surface-displayed FRET nanosensors. Proceedings of the National Academy of Sciences **102:** 8740-8745

Okumoto S, Takanaga H, Frommer WB (2008) Quantitative imaging for discovery and assembly of the metabo-regulome. New Phytologist **180:** 271-295

Persechini A, Lynch JA, Romoser VA (1997) Novel fluorescent indicator proteins for monitoring free intracellular Ca^{2+}. Cell Calcium **22:** 209-216

Piljic A, Schultz C (2008) Simultaneous recording of multiple cellular events by FRET. ACS Chemical Biology **3:** 156-160

Plaxton WC, Carswell MC (1999) Metabolic aspects of the phosphate starvation response in plants. *In* HR Lerner, ed, Plant Responses to Environmental Stresses: From Phytohormones to Genome Reorganization. M. Dekker, New York, NY, USA, pp 350-372

Plaxton WC, Tran HT (2011) Metabolic adaptations of phosphate-starved plants. Plant Physiology **156:** 1006-1015

Pocker Y, Janjic N (1987) Enzyme kinetics in solvents of increased viscosity. Dynamics aspects of carbonic anhydrase catalysis. Biochemistry **26:** 2597-2606

Poirier Y, Bucher M (2002) Phosphate transport and homeostasis in Arabidopsis. *In* CR Somerville, EM Meyerowitz, eds, The Arabidopsis Book, doi/10.1199/tab.0024, American Society of Plant Biologists, Rockville, MD, USA, pp 1-35

Pratt J, Boisson A-M, Gout E, Bligny R, Douce R, Aubert S (2009) Phosphate (Pi) starvation effect on the cytosolic Pi concentration and Pi exchanges across the tonoplast in plant cells: An in Vivo 31P-Nuclear Magnetic Resonance Study Using Methylphosphonate as a Pi Analog. Plant Physiology **151:** 1646-1657

Preiss J (1982) Regulation of the biosynthesis and degradation of starch. Annual Review of Plant Biology **33:** 431-454

Raghothama K (1999) Phosphate acquisition. Annual Review of Plant Physiology and Plant Molecular Biology **50:** 665-693

Ratcliffe RG, Shachar-Hill Y (2001) Probing plant metabolism with NMR. Annual Review of Plant Physiology and Plant Molecular Biology **52:** 499-526

Rausch C, Bucher M (2002) Molecular mechanisms of phosphate transport in plants. Planta **216:** 23-37

Rausch C, Zimmermann P, Amrhein N, Bucher M (2004) Expression analysis suggests novel roles for the plastidic phosphate transporter Pht2;1 in auto- and heterotrophic tissues in potato and Arabidopsis. Plant Journal **39:** 13-28

Rebeille F, Bligny R, Douce R (1984) Is the Cytosolic Pi Concentration a Limiting Factor for Plant Cell Respiration? Plant Physiology **74:** 355-359

Reinhold T, Alawady A, Grimm B, Beran KC, Jahns P, Conrath U, Bauer J, Reiser J, Melzer M, Jeblick W, Neuhaus HE (2007) Limitation of nocturnal import of ATP into Arabidopsis chloroplasts leads to photooxidative damage. Plant Journal **50:** 293-304

Reiser J, Linka N, Lemke L, Jeblick W, Neuhaus HE (2004) Molecular physiological analysis of the two plastidic ATP/ADP transporters from Arabidopsis. Plant Physiology **136:** 3524-3536

Renne P, Dressen U, Hebbeker U, Hille D, Flugge UI, Westhoff P, Weber AP (2003) The Arabidopsis mutant *dct* is deficient in the plastidic glutamate/malate translocator DiT2. Plant Journal **35:** 316-331

Riesmeier JW, Flügge UI, Schulz B, Heineke D, Heldt HW, Willmitzer L, Frommer WB (1993) Antisense repression of the chloroplast triose phosphate translocator affects carbon partitioning in transgenic potato plants. Proceedings of the National Academy of Sciences **90:** 6160-6164.

Rincon-Zachary M, Teaster ND, Sparks JA, Valster AH, Motes CM, Blancaflor EB (2010) Fluorescence resonance energy transfer-sensitized emission of yellow cameleon 3.60 reveals root zone-specific calcium signatures in Arabidopsis in response to aluminum and other trivalent cations. Plant Physiology **152:** 1442-1458

Robinson D (1994) The responses of plants to non-uniform supplies of nutrients. New Phytologist **127:** 635-674

Robinson WD, Carson I, Ying S, Ellis K, Plaxton WC (2012) Eliminating the purple acid phosphatase AtPAP26 in *Arabidopsis thaliana* delays leaf senescence and impairs phosphorus remobilization. New Phytologist **196:** 1024-1029

Roszik J, Szollosi J, Vereb G (2008) AccPbFRET: an ImageJ plugin for semi-automatic, fully corrected analysis of acceptor photobleaching FRET images. BioMedCentral Bioinformatics **9:** 346**:**1-6

Roth C, Menzel G, Petetot JM, Rochat-Hacker S, Poirier Y (2004) Characterization of a protein of the plastid inner envelope having homology to animal inorganic phosphate, chloride and organic-anion transporters. Planta **218:** 406-416

Rouached H, Arpat AB, Poirier Y (2010) Regulation of phosphate starvation responses in plants: Signaling Players and Cross-Talks. Molecular Plant **3:** 288-299

Ruiz Pavón L, Lundh F, Lundin B, Mishra A, Persson BL, Spetea C (2008) ANTR1 is a thylakoid Na^+-dependent phosphate transporter: functional characterization in *Escherichia coli*. Journal of Biological Chemistry **283:** 13520-13527

Sánchez-Calderón L, López-Bucio J, Chacón-López A, Cruz-Ramírez A, Nieto-Jacobo F, Dubrovsky JG, Herrera-Estrella L (2005) Phosphate starvation induces a determinate developmental program in the roots of *Arabidopsis thaliana*. Plant and Cell Physiology **46:** 174-184

Schachtman DP, Reid RJ, Ayling SM (1998) Phosphorus uptake by plants: from soil to cell. Plant Physiology **116:** 447-453

Schneider A, Häusler RE, Kolukisaoglu Ü, Kunze R, van der Graaff E, Schwacke R, Catoni E, Desimone M, Flügge UI (2002) An *Arabidopsis thaliana* knock-out mutant of the chloroplast triose phosphate/phosphate translocator is severely compromised only when starch synthesis, but not starch mobilisation is abolished. Plant Journal **32:** 685-699

Shaner NC, Steinbach PA, Tsien RY (2005) A guide to choosing fluorescent proteins. Nature Methods **2:** 905-909

Sharkey TD (1985) Photosynthesis in intact leaves of C3 plants: physics, physiology and rate limitations. Botanical Review **51:** 53-105

Sharkey TD, Vanderveer PJ (1989) Stromal phosphate concentration is low during feedback limited photosynthesis. Plant Physiology **91:** 679-684

Sharkey TD, Bernacchi CJ, Farquhar GD, Singsaas EL (2007) Fitting photosynthetic carbon dioxide response curves for C(3) leaves. Plant, Cell & Environment **30:** 1035-1040

Shcherbo D, Souslova E, Goedhart J, Chepurnykh T, Gaintzeva A, Shemiakina I, Gadella T, Lukyanov S, Chudakov D (2009) Practical and reliable FRET/FLIM pair of fluorescent proteins. BioMedCentral Biotechnology **9:** 24

Sheu-Hwa C-S, Lewis DH, Walker DA (1975) Stimulation of photosynthetic starch formation by sequestration of cytoplasmic orthophosphate. New Phytologist **74:** 383-392

Shingles R, McCarty RE (1995) Production of membrane vesicles by extrusion: size distribution, enzyme activity, and orientation of plasma membrane and chloroplast inner-envelope membrane vesicles. Analalytical Biochemistry **229:** 92-98

Shingles R, North M, McCarty RE (2001) Direct measurement of ferrous ion transport across membranes using a sensitive fluorometric assay. Analytical Biochemistry **296:** 106-113

Shingles R, North M, McCarty RE (2002) Ferrous ion transport across chloroplast inner envelope membranes. Plant Physiology **128:** 1022-1030

Shingles R, Roh MH, McCarty RE (1996) Nitrite transport in chloroplast inner envelope vesicles (I. Direct Measurement of Proton-Linked Transport). Plant Physiology **112:** 1375-1381

Sivak MN, Walker DA (1986) Photosynthesis *in vivo* can be limited by phosphate supply. New Phytologist **102:** 499-512

Smith AM, Stitt M (2007) Coordination of carbon supply and plant growth. Plant, Cell & Environment **30:** 1126-1149

Smith AM, Zeeman SC (2006) Quantification of starch in plant tissues. Nature Protocols **1:** 1342-1345

Smith AP, Jain A, Deal RB, Nagarajan VK, Poling MD, Raghothama KG, Meagher RB (2010) Histone H2A.Z regulates the expression of several classes of

phosphate starvation response genes but not as a transcriptional activator. Plant Physiology **152:** 217-225

Smith FW, Jackson WA, van den Berg PJ (1990) Internal phlosphorus flows during development of phosphorus stress. Australian Journal of Plant Physiology **17:** 451-464

Socolich M, Lockless SW, Russ WP, Lee H, Gardner KH, Ranganathan R (2005) Evolutionary information for specifying a protein fold. Nature **437:** 512-518

Soumpasis DM (1983) Theoretical analysis of fluorescence photobleaching recovery experiments. Biophysical Journal **41:** 95-97

Stitt M, Wilke I, Feil R, Heldt H (1988) Coarse control of sucrose-phosphate synthase in leaves: Alterations of the kinetic properties in response to the rate of photosynthesis and the accumulation of sucrose. Planta **174:** 217-230

Takabatake R, Hata S, Taniguchi M, Kouchi H, Sugiyama T, Izui K (1999) Isolation and characterization of cDNAs encoding mitochondrial phosphate transporters in soybean, maize, rice, and Arabidopis. Plant Molecular Biology **40:** 479-486

Takizawa K, Kanazawa A, Kramer DM (2008) Depletion of stromal P_i induces high 'energy-dependent' antenna exciton quenching (q_E) by decreasing proton conductivity at CF_o-CF_1 ATP synthase. Plant, Cell & Environment **31:** 235-243

Tam R, Saier MH (1993) Structural, functional, and evolutionary relationships among extracellular solute-binding receptors of bacteria. Microbiological Reviews **57:** 320-346

Tiessen A, Nerlich A, Faix B, Hummer C, Fox S, Trafford K, Weber H, Weschke W, Geigenberger P (2012) Subcellular analysis of starch metabolism in developing barley seeds using a non-aqueous fractionation method. Journal of Experimental Botany **63:** 2071-2087

Tramier M, Zahid M, Mevel J-C, Masse M-J, Coppey-Moisan M (2006) Sensitivity of CFP/YFP and GFP/mCherry pairs to donor photobleaching on FRET determination by fluorescence lifetime imaging microscopy in living cells. Microscopy Research and Technique **69:** 933-939

Truernit E, Haseloff J (2008) A simple way to identify non-viable cells within living plant tissue using confocal microscopy. Plant Methods **4:** 1-15

Versaw WK, Harrison MJ (2002) A chloroplast phosphate transporter, PHT2;1, influences allocation of phosphate within the plant and phosphate-starvation responses. Plant Cell **14:** 1751-1766

Vidal G, Gallis JL, Dufour S, Canioni P (1997) NMR studies of inorganic phosphate compartmentation in the isolated rat liver during acidic perfusion. Archives of Biochemistry and Biophysics **337:** 317-325

Walker DA, Sivak MN (1986) Photosynthesis and phosphate: a cellular affair? Trends in Biochemical Sciences **11:** 176-179

Walters RG, Ibrahim DG, Horton P, Kruger NJ (2004) A mutant of Arabidopsis lacking the triose-phosphate/phosphate translocator reveals metabolic regulation of starch breakdown in the light. Plant Physiology **135:** 891-906

Weber AP (2004) Solute transporters as connecting elements between cytosol and plastid stroma. Current Opinion in Plant Biology **7:** 247-253

Weber AP, Linka N (2011) Connecting the plastid: transporters of the plastid envelope and their role in linking plastidial with cytosolic metabolism. Annual Review of Plant Biology **62:** 53-77

Weber AP, Schneidereit J, Voll LM (2004) Using mutants to probe the in vivo function of plastid envelope membrane metabolite transporters. Journal of Experimental Botany **55:** 1231-1244

Whatley JM (1978) A suggested cycle of plastid developmental interrelationships. New Phytologist **80:** 489-502

Woodrow I, Raymond Ellis J, Jellings A, Foyer C (1984) Compartmentation and fluxes of inorganic phosphate in photosynthetic cells. Planta **161:** 525-530

Wu W, Peters J, Berkowitz GA (1991) Surface charge-mediated effects of Mg^{2+} on K^{+} flux across the chloroplast envelope are associated with regulation of stromal pH and photosynthesis. Plant Physiology **97:** 580-587

Yang H, Bogner M, Stierhof Y-D, Ludewig U (2010) H+independent glutamine transport in plant root tips. PLoS ONE **5:** 008917**:** 1-9

Yoo SD, Cho YH, Sheen J (2007) Arabidopsis mesophyll protoplasts: a versatile cell system for transient gene expression analysis. Nature Protocols **2:** 1565-1572

Zhao L, Versaw WK, Liu J, Harrison MJ (2003) A phosphate transporter from *Medicago truncatula* is expressed in the photosynthetic tissues of the plant and is located in the chloroplast envelope. New Phytologist **157:** 291-302